OPEN ACCESS

Original research

Secondary bile acid production by gut bacteria promotes Western diet-associated colorectal cancer

Annika Osswald ,[1,2] Esther Wortmann,[3] David Wylensek,[3] Stephanie Kuhls,[4] Olivia I Coleman,[4] Kenneth Peuker,[5] Anne Strigli,[5] Quinten R Ducarmon,[6] Martin Larralde,[6,7] Wei Liang,[8,9] Nicole S Treichel,[3] Fabian Schumacher ,[10] Colin Volet,[11] Silke Matysik,[12] Karin Kleigrewe,[13] Michael Gigl,[13] Sascha Rohn,[14] Chun-Jun Guo,[15] Burkhard Kleuser,[10] Gerhard Liebisch,[12] Angelika Schnieke,[8] Jason M Ridlon,[16] Rizlan Bernier-Latmani,[11] Georg Zeller ,[6,7] Sebastian Zeissig,[5,17] Dirk Haller ,[4,18] Krzysztof Flisikowski,[8,9] Thomas Clavel ,[3] Soeren Ocvirk[1,2]

► Additional supplemental material is published online only. To view, please visit the journal online (https://doi.org/10.1136/gutjnl-2024-332243).

For numbered affiliations see end of article.

Correspondence to
Professor Thomas Clavel; tclavel@ukaachen.de and Dr. Soeren Ocvirk; soeren.ocvirk@dife.de; soeren.ocvirk@tum.de

AO and EW are joint first authors.
TC and SO are joint senior authors.

Received 26 February 2024
Accepted 13 November 2025
Published Online First
18 December 2025

Check for updates

© Author(s) (or their employer(s)) 2026. Re-use permitted under CC BY-NC. No commercial re-use. See rights and permissions. Published by BMJ Group.

To cite: Osswald A, Wortmann E, Wylensek D, *et al*. *Gut* 2026;**75**:1505–1519.

ABSTRACT

Background Western diet and associated production of secondary bile acids (BAs) have been linked to the development of sporadic colorectal cancer (CRC). Despite observational studies showing that secondary BAs produced by 7α-dehydroxylating (7αDH+) gut bacteria are increased in CRC, a causal proof of their tumour-promoting effects is lacking.

Objective Investigate the causal role of BAs produced by 7αDH+ gut bacteria in CRC.

Design We performed feeding studies in a porcine model of CRC combined with multi-omics analyses and gnotobiotic mouse models colonised with 7αDH+ bacteria or a genetically modified strain to demonstrate causality.

Results Western diet exacerbated the CRC phenotype in *APC*$^{1311/+}$ pigs. This was accompanied by increased levels of the secondary BA deoxycholic acid (DCA) and higher colonic epithelial cell proliferation. The latter was counteracted by the BA-scavenging drug colestyramine. Metagenomic analysis across multiple human cohorts revealed higher occurrence of *bai* (BA inducible) operons from *Clostridium scindens* and close relatives in faeces of patients with CRC. Addition of these specific 7αDH+ bacteria (*C. scindens*/*Extibacter muris*) to defined communities of gut bacteria led to DCA production and increased colon tumour burden in mouse models of chemically or genetically induced CRC. A mutant strain of *Faecalicatena contorta* lacking 7αDH caused fewer colonic tumours in azoxymethane/dextran sodium sulfate treated mice and triggered less epithelial cell proliferation in human colon organoids compared with wild-type *F. contorta*.

Conclusion This work provides functional evidence for the causal role of secondary BAs produced by gut bacteria through 7αDH in CRC under adverse dietary conditions, opening avenues for future preventive strategies.

WHAT IS ALREADY KNOWN ON THIS TOPIC

⇒ Western diet has been linked to the development of sporadic colorectal cancer (CRC).
⇒ Dietary fat stimulates the production of secondary bile acids (BAs) by 7α-dehydroxylating (7αDH+) bacteria within the gut microbiome.
⇒ Functional studies demonstrating a causal role of 7αDH+ bacteria in CRC are lacking.

WHAT THIS STUDY ADDS

⇒ Western diet exacerbates experimental colorectal tumourigenesis in *APC*$^{1311/+}$ pigs, providing interventional proof for associative clinical data in a relevant preclinical model.
⇒ Enhanced epithelial cell proliferation is associated with increased levels of faecal secondary BAs, particularly deoxycholic acid (DCA), and can be reversed by colestyramine administration in pigs.
⇒ Colonisation of gnotobiotic mice with specific 7αDH+ bacteria induces DCA production, stimulates colonic epithelial cell proliferation and alters the expression of genes involved in epithelial cell differentiation.
⇒ 7αDH+ bacteria increased colon tumour burden in two gnotobiotic CRC models, while a 7αDH− mutant strain did not, demonstrating a causal role in experimental colon tumourigenesis.

HOW THIS STUDY MIGHT AFFECT RESEARCH, PRACTICE OR POLICY

⇒ The causal role of elevated levels of secondary BAs, particularly DCA, in Western diet-associated colonic tumourigenesis supports the implementation of personalised dietary interventions to reduce the production of secondary BAs in individuals at risk of CRC.
⇒ Specific detection of *Clostridium scindens* and closely related 7αDH+ species in human stool may help to identify individuals at high risk of CRC associated with adverse diet and lifestyle.
⇒ Future microbiome-based interventions for CRC prevention (new onset or post surgery) should explore targeting specific 7αDH+ bacteria.

INTRODUCTION

Colorectal cancer (CRC) has one of the highest incidences and mortalities among all cancer types worldwide, with approximately 1.9 million new cases and 0.9 million deaths in 2022.[1] Besides genetic factors, including mutations in the

Gut: first published as 10.1136/gutjnl-2024-332243 on 18 December 2025. Downloaded from http://gut.bmj.com/ on November 19, 2026 by guest. Protected by copyright, including for uses related to text and data mining, AI training, and similar technologies.

tumour-suppressing adenomatous polyposis coli (*APC*) gene, sporadic CRC risk is predominantly influenced by environmental and lifestyle factors, including diet and the gut microbiome.[2 3] There is convincing evidence for a positive association between CRC risk and Western-style diets rich in fat and red/processed meat, while high-fibre intake is negatively associated with CRC risk. In healthy individuals in South Africa, who have a very low CRC risk, a diet switch for 2 weeks from a traditional high-fibre/low-fat to a Western-style low-fibre/high-fat diet altered gut microbiota composition and metabolism, leading to an increase in markers associated with CRC risk such as intestinal epithelial cell (IEC) proliferation and infiltration of CD3+ and CD68+ immune cells.[4] Alaskan Native people, who traditionally consume a diet rich in fat and have the world's highest risk for CRC, have a gut microbiota characterised by lower diversity and metabolic adaption to bile acid (BA) metabolism.[5]

High-fat intake stimulates BA synthesis by the host, resulting in increased amounts of BAs entering the colon, where they are converted to secondary BAs by gut bacteria. Elevated levels of secondary BAs, in particular deoxycholic acid (DCA), were detected in faeces of patients with CRC and healthy individuals at high CRC risk, and they correlated with higher occurrence of BA-inducible (*bai*) genes involved in BA 7α-dehydroxylation (7αDH) by gut bacteria.[4–7] In the murine $Apc^{min/+}$ model, a diet supplemented with the primary BA cholic acid (CA, 0.4% w/w, 12 weeks), the precursor of DCA, increased the number and size of intestinal tumours.[8] This effect was prevented by antibiotic treatment, suggesting a contribution of the gut microbiota to CA-associated tumourigenesis in this CRC model. Oral intake of DCA promoted tumour development in the proximal colon of wild-type mice (0.2% w/w in diet for up to 10 months),[9] high-grade dysplasia in AKR/J mice treated with azoxymethane (AOM) (0.25% w/w in diet for >10 weeks)[10] and higher numbers of intestinal tumours in $Apc^{min/+}$ mice (0.2% w/v in drinking water for 12 weeks).[11] Faecal microbiota transplantation from DCA-treated $Apc^{min/+}$ donor mice to microbiota-depleted $Apc^{min/+}$ recipients on a control diet led to increased intestinal tumour numbers.[12] However, in these studies, mice were fed with DCA directly, which does not mirror physiological conditions, or DCA levels were not analysed. Moreover, the $Apc^{min/+}$ mouse model develops tumours primarily in the small intestine, which does not reflect the location of tumourigenesis in humans and contrasts to colon being the main site of secondary BAs production. Hence, clear evidence for a causal role of microbially produced DCA in relation to diet and underlying mechanisms in colonic tumourigenesis is lacking.

In this study, we investigated the role of secondary BA production by gut bacteria in CRC, based on a multilayer approach using dietary interventions in genetically engineered pigs, patient stool samples, gnotobiotic mouse models of CRC, human colon organoids, and a combination of multi-omics and cultivation methods. This allowed us to span analyses from microbial community level to detailed investigations of specific microbiota members involved in the conversion of BAs, collectively demonstrating a diet-driven, tumour-promoting function of secondary BA-producing bacteria.

RESULTS

Western diet promotes high levels of secondary BAs and aggravates disease in $APC^{1311/+}$ pigs

Pigs and humans are omnivores and share similarities in their gut microbiota, gastrointestinal anatomy, physiology and metabolic processes. This has made the pig an ideal model to study gastrointestinal diseases. In contrast to transgenic mouse models based on mutations of the *Apc* gene, $APC^{1311/+}$ pigs recapitulate key features of human disease, including the location of tumours in the large intestine,[13] disease progression and differences in severity within families.[14]

To investigate the role of a Western diet on the development of CRC under controlled conditions in a preclinical setting, we performed a feeding intervention in $APC^{1311/+}$ pigs. The animals were fed (1 kg/day) either a control (CTRL) diet or an experimental diet enriched in red meat and lard (RL diet) for 3 months (see experimental design in online supplemental figure S1a and diet composition in online supplemental table S1). Compared with control $APC^{1311/+}$ pigs, higher numbers of Ki67+ (marker for cell proliferation) cells in distal colonic crypts indicated increased proliferation of the colonic epithelium in the RL diet group (figure 1a), which was accompanied by a significant increase in both the number and size of colonic polyps (figure 1b).

To assess the effects of experimental feeding on the gut microbial ecosystem, faecal samples were analysed by 16S rRNA gene amplicon sequencing before and after intervention. *Alpha*-diversity analysis revealed a trend towards increased richness and Shannon effective counts in the CTRL group, which was not observed in the RL group, including a sharp drop in diversity in the two pigs with most severe disease progression (figure 1c). According to *beta*-diversity analysis, the microbiota structure between CTRL and RL pigs overlapped at the beginning of the feeding trial (4 months) but diverged after experimental feeding (7 months, figure 1d). At the level of dominant bacterial families, a decrease in *Prevotellaceae* and *Acidaminococcaceae* over time was observed in both groups, but it was more pronounced in RL pigs (figure 1e). While *Fibrobacteraceae* increased in the CTRL group, RL pigs were characterised by a significant increase in *Desulfovibrionaceae*.

Besides diet-induced effects on microbiota diversity and composition, changes in faecal metabolites were assessed. Targeted liquid chromatography with tandem mass spectrometry (LC-MS/MS) measurements showed that primary BAs were overall increased in RL pigs after dietary intervention, primarily due to glycocholic acid (GCA), which was not detected in the CTRL group (figure 1f). Total faecal concentrations of secondary BAs were slightly higher in the CTRL group, mainly driven by hyodeoxycholic acid, which was shown by others to suppress epithelial cell proliferation.[15] In contrast, levels of the CRC-associated secondary BAs DCA and 12-keto-litocholic acid (12-KLCA) were substantially higher in the RL group (figure 1g).

The bile acid sequestrant colestyramine limits Western diet-associated epithelial cell proliferation in the colon of $APC^{1311/+}$ pigs

Next, we investigated whether the increase in BAs contributed to the RL diet-induced phenotype in $APC^{1311/+}$ pigs. To this end, a second feeding trial was carried out, including a third group fed the RL diet supplemented with the drug colestyramine (COL; 12 g/day), a bile acid scavenger that enhances bile acids excretion in faeces[16] (see experimental design in online supplemental figure S1b). Immunohistochemistry staining of Ki67+ cells confirmed the proliferative effect of the RL diet in crypts of the distal colon, which was prevented by COL in the normal mucosa (figure 2a) and in lesions (online supplemental figure S2). While the number of polyps tended to decrease after intervention in all COL pigs (figure 2b; p=0.062), their size varied markedly between individuals in this group (figure 2c). Moreover, the total number and

Gut: first published as 10.1136/gutjnl-2024-332243 on 18 December 2025. Downloaded from http://gut.bmj.com/ on November 19, 2026 by guest. Protected by copyright, including for uses related to text and data mining, AI training, and similar technologies.

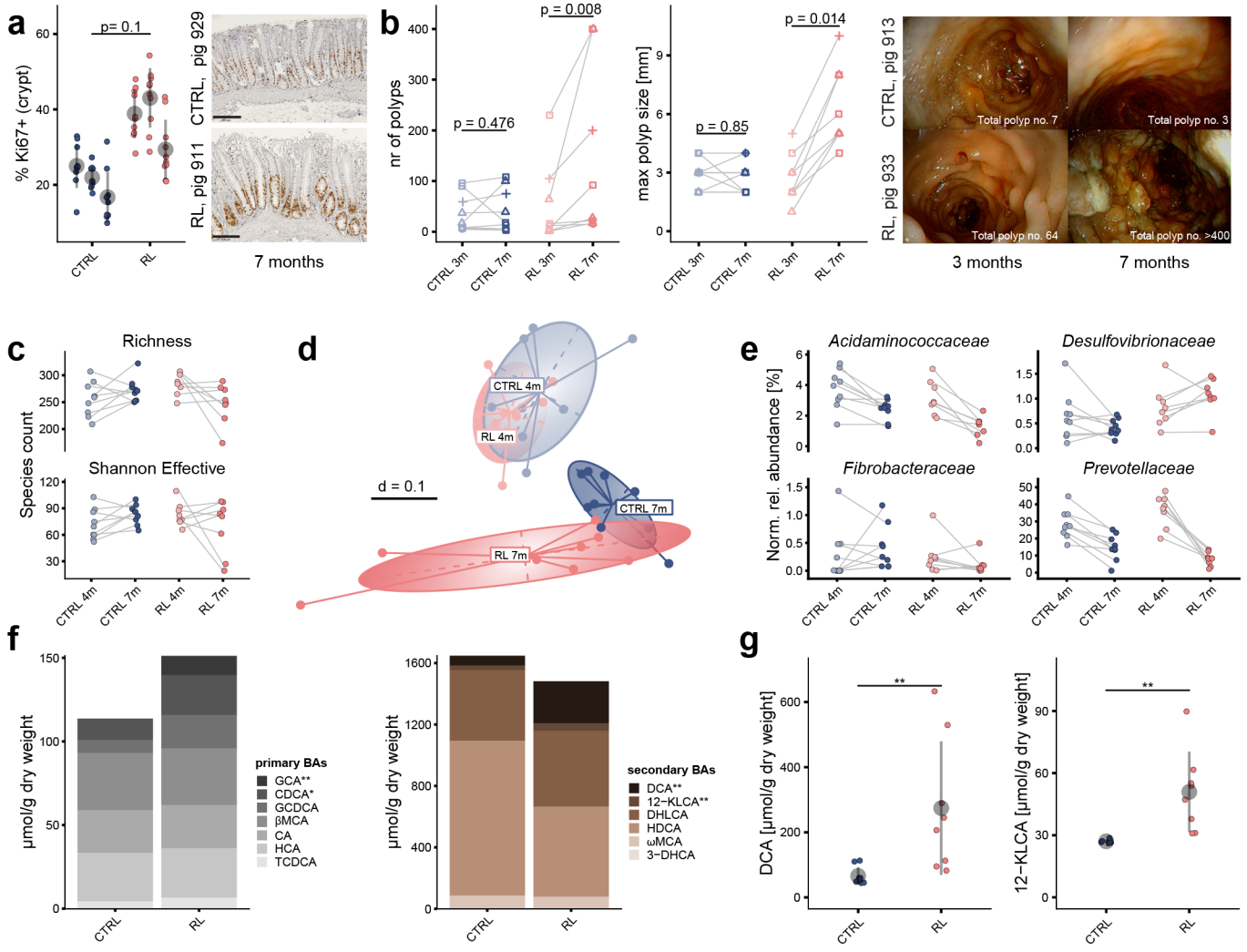


Figure 1 Effects of Western diet on disease phenotype, faecal microbiota (16S rRNA amplicon sequencing) and bile acids (LC-MS/MS): (a) Percentage of Ki67+ cells in crypts of the distal colon from CTRL and RL pigs (n=3 each) after the feeding intervention; for each pig, 10 randomly selected fields were counted (small coloured dots). Mean values and SD per pig are shown in grey. Right panel: Exemplary Ki67 staining of distal colon samples. Black bars on the pictures represent 200 µm. (b) Number and size of polyps in the distal colon of *APC*$^{1311/+}$ pigs aged 3 months (1 month prior to the feeding intervention) or 7 months (end of feeding intervention) and fed either the red meat and lard diet (n=8; red symbols) or the control diet (n=9; blue). Litters are indicated by different symbols. Right panel: Exemplary endoscopic pictures (last 40 cm of the colon). (c) Richness and Shannon effective counts over time; p=0.0206 and 0.1390, respectively (comparison of delta values). 4 months is the start of the dietary intervention, 7 months the end. (d) *Beta*-diversity shown as metaNMDS plot of generalised Unifrac distances. (e) Relative abundances of dominant bacterial families with significantly different changes over time (end-start/start) between feeding groups; (f) primary (grey stack bars) and secondary (brown) BA levels in faeces at the end of the feeding period; mean values per feeding group are shown (n=9 for CTRL, n=8 for RL). All values are available in online supplemental table S2. (g) Dot plots of the secondary BAs DCA and 12-KLCA in faeces. Mean values and SD across all pigs per group are shown in grey. Statistics: (a) Unpaired Wilcoxon rank-sum test; (b) Paired Wilcoxon signed-rank test; (d) PERMANOVA, p=0.001; pairwise comparisons with Benjamini-Hochberg adjustment: start, p.adj.=0.399; end, p.adj.=0.0015. (c–g) Wilcoxon rank-sum test with Benjamini-Hochberg adjustment (*p.adj.≤0.05, **p.adj.≤0.01). BAs, bile acids; CA, cholic acid; CDCA, chenodeoxycholic acid; CTRL, control; DCA, deoxycholic acid; DHCA, dehydrocholic acid; DHLCA, dehydro-lithocholic acid; GCA, glycocholic acid; GCDCA, glycochenodeoxycholic acid; HCA, hyocholic acid; HDCA, hyo-deoxycolic acid; KLCA, keto-litocholic acid; Ki67, marker for cell proliferation; LC-MS/MS, liquid chromatography with tandem mass spectrometry; metaNMDS, meta non-metric multidimensional scaling; m, month; MCA, muricholic acid; norm. rel., normalised relative; nr, number; p.adj., adjusted p value; PERMANOVA, permutational multivariate analysis of variance; RL, red meat and lard diet; TCDCA, tauro-chenodeoxycholic acid.

size of polyps in the CTRL and RL groups showed inconsistent changes over time. However, compared with the RL diet, treatment with COL resulted in fewer progressing polyps (figure 2d). Targeted analysis of faecal BAs at the end of the feeding period showed higher total levels of primary and secondary BAs in RL and COL pigs (adjusted p value (p.adj.)=0.068 and 0.066, respectively), including higher concentrations of GCA (p.adj.=0.05), allocholic acid (p.adj.=0.07), CA and ursocholic acid (p.adj.=0.05) (figure 2e). Faecal concentrations of the secondary BAs DCA and 12-KLCA increased with RL diet feeding, while they tended to be lower under COL treatment, even though these faecal amounts do not reflect the levels to which the gut epithelium is exposed (figure 2f). Targeted measurements of BAs were complemented by a lipidomics approach. Levels of

Gut: first published as 10.1136/gutjnl-2024-332243 on 18 December 2025. Downloaded from http://gut.bmj.com/ on November 19, 2026 by guest. Protected by copyright, including for uses related to text and data mining, AI training, and similar technologies.

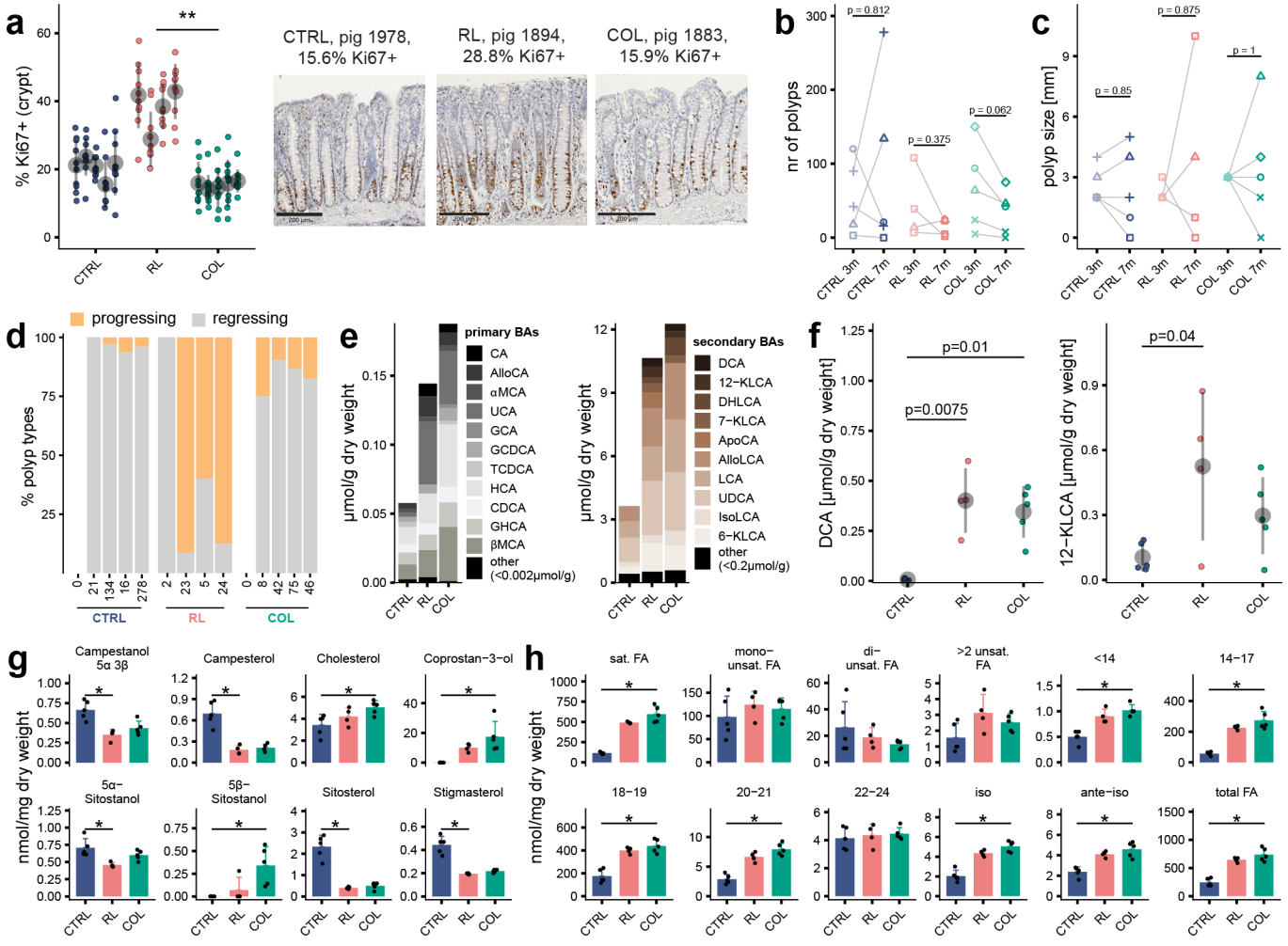


Figure 2 Colestyramine treatment in transgenic *APC*$^{1311/+}$ pigs: The COL diet corresponded to RL diet supplemented with 12 g/kg colestyramine (see detailed composition in online supplemental table S1). (a) Percentage of Ki67+ cells in crypts of the distal colon. For each pig, 10 randomly selected fields were counted (coloured dots). Mean values and SD per pig are shown in grey. Exemplary microscopic pictures of Ki67 staining (bars=200 µm) are displayed next to the graph. Polyp number (b) and size (c) in the distal colon (last 40 cm, 1 month prior to intervention; end of feeding period, n=5 for CTRL and COL, n=4 for RL). Litters are indicated by different symbols. (d) Fraction of progressing or regressing polyps (see Methods) as percentage of total polyp numbers (indicated below the x-axis for each pig). (e) Mean values of primary (grey) and secondary (brown) BAs at the end of the feeding period (7 months). All values are given in online supplemental table S3. (f) Individual values for DCA and 12-KLCA. Mean values and SD are shown in grey. (g) Sterol/stanol profiles. (h) FA profiles: total sat. FA, monounsaturated FA, di-unsaturated FA, >2 unsaturated FA, FAs separated by chain length, branched chain FA (iso- and ante-iso) and total FA. Individual values are provided in online supplemental table S3. Values in (g and h) are shown as individual values (black dots) and mean (bars)+SD (whiskers). CTRL diet (n=5); RL diet (n=4); COL diet (n=5). Statistics: (b and c) Paired Wilcoxon signed-rank test; (a, e–h) Kruskal-Wallis test with Dunn's multiple comparisons and Benjamini-Hochberg adjustment (*p. adj.≤0.05). (d) Pearson's χ^2. AlloCA, allocholic acid; AlloLCA; allolithocholic acid; ApoCA, apocholic acid; BAs, bile acids; CA, cholic acid; CDCA, chenodeoxycholic acid; COL, colestyramine; CTRL, control; DCA, deoxycholic acid; DHCA, dehydrocholic acid; DHLCA, dehydro-lithocholic acid; FA, fatty acid; GCA, glycocholic acid; GCDCA, glycochenodeoxycholic acid; GHCA, glycohyocholic acid; HCA, hyocholic acid; IsoLCA, isolithocholic acid; KLCA, keto-litocholic acid; Ki67, marker for cell proliferation; LCA, lithocholic acid; m, month; MCA, muricholic acid; nr, number; RL, red meat and lard diet; sat. saturated; TCDCA, tauro-chenodeoxycholic acid; UCA, ursocholic acid; UDCA, ursodeoxycholic acid; unsat., unsaturated.

plant sterols were elevated in faecal samples from CTRL pigs, and COL tended to compensate for this effect in the case of cholestanol and 5α-sitostanol (figure 2g). In contrast, the levels of cholesterol and derivatives as well as total fatty acids (FAs) were highest in faeces of COL pigs (figure 2h). The differences in FAs were mainly driven by total saturated and branched chain (iso and ante-iso) FA, whereas unsaturated and long-chain FA (22–24) showed no significant differences.

Taken together, the two feeding trials in genetically engineered pigs provide interventional evidence for the positive association between Western dietary habits, elevated levels of secondary BAs and polyp formation. Western diet-driven epithelial cell proliferation in the colon was prevented by the drug COL, which stimulated faecal excretion of lipids, making them likely unavailable for the host and BAs not accessible for bacterial conversion into secondary BAs. To further demonstrate the causal implication of secondary BAs in CRC development, we next used gnotobiotic mouse models.

Specific 7αDH+ bacteria are associated with CRC

Given the diversity of *Clostridium* and related species encoding *bai* genes, we next sought to identify the most relevant 7αDH+ bacteria in the context of CRC and explore their roles in

Gut: first published as 10.1136/gutjnl-2024-332243 on 18 December 2025. Downloaded from http://gut.bmj.com/ on November 19, 2026 by guest. Protected by copyright, including for uses related to text and data mining, AI training, and similar technologies.

functional experiments. Therefore, we analysed the occurrence of *bai* operons from different mOTUs (metagenomic operational taxonomic units) in faecal metagenomes from patients with CRC (n=1034) and control individuals (n=1108) across multiple cohorts.[17] The seven mOTUs with a prevalence >2% showed specificity in terms of both *bai* operon structure and protein sequence comparison (figure 3a,b). The occurrence of only two mOTUs corresponding to cultured species, *Clostridium scindens* (r03437) and *C. hylemonae* (r11469), was significantly higher in patients with CRC (figure 3c). Cumulative relative abundances of the *bai* operons from *C. scindens* and *C. hylemonae* confirmed the relevance of these two species in CRC when analysing all cohorts together (figure 3d). An increase was observed in nearly all individual studies, but significance depended on the cohort considered, likely due to varying size and environmental parameters (eg, diet) (figure 3e).

Based on the aforementioned metagenomic data, we used *C. scindens* in a gnotobiotic mouse model to study the relevance of microbial DCA production in CRC development. Germ-free wild-type mice on a high-fat diet (HFD) were colonised with a simplified consortium of human gut bacteria referred to as 'BA-converting defined microbiota' (BACOMI) (online supplemental figure S1c,d). BACOMI includes 7αDH+ activity by *C. scindens* to produce DCA and can be compared with the condition without DCA when *C. scindens* is excluded from the consortium (7αDH−). Targeted quantitative PCR (qPCR) analysis revealed a high relative abundance of 23.0±2.9% (mean±SD) for *C. scindens* in BACOMI-colonised mice and a relatively uniform colonisation pattern of the other bacteria after 3 months (figure 3f). Consistently, the presence of *C. scindens* caused high levels of secondary BAs, in particular DCA, which was not detected when 7αDH activity was lacking in the microbial consortium (figure 3g and online supplemental figure S3a). DCA concentrations were higher in female than male mice when colonised by *C. scindens*. Interestingly, 7αDH activity and DCA enhanced the expression of genes within BA-dependent signalling pathways (figure 3h) or involved in epithelial cell function and tumourigenesis in the colonic epithelium (figure 3i). Furthermore, 7αDH activity was linked to higher numbers of Ki67+ epithelial cells in the colon (figure 3j). Consistently, DCA induced epithelial cell proliferation in human colon organoids compared with CA (online supplemental figure S4a) or when added to supernatants of BACOMI, with or without *C. scindens*, excluding potential confounding factors due to other bacterial stimuli (online supplemental figure S4b,c).

Microbially produced deoxycholic acid promotes tumourigenesis in the colon

To analyse whether 7αDH-mediated BAs affect colonic tumourigenesis, germ-free wild-type mice on HFD were colonised with BACOMI with or without *C. scindens* and then treated with AOM and dextran sodium sulfate (DSS) (figure 4a). To consolidate these findings independent of the 7αDH+ bacterial species used, we performed additional experiments in mice colonised with the mouse gut isolate *Extibacter muris*[18] instead of *C. scindens*. The *bai* operon of *E. muris* has a high similarity to the *bai* operon of *C. hylemonae*[18] and the latter species was also significantly associated with CRC in the metagenomic analysis (figure 3c). Moreover, *C. hylemonae* is proposed to be reclassified within the genus *Extibacter* in GTDB (Release R226),[19] highlighting the phylogenetic relatedness of these two species.

Following AOM/DSS treatment, *C. scindens* was present at higher relative abundance (50.3±7.1%) (figure 4b) when compared with untreated BACOMI-colonised mice (figure 3f), suggesting favourable growth conditions for *C. scindens* under chemically induced colonic tumourigenesis. DCA was only detected in gnotobiotic mice colonised with *C. scindens*, including higher levels in female mice (figure 4d and online supplemental figure S5a). Levels of 3-oxo-DCA were also higher in the caecal content of female mice when *C. scindens* was present. Despite these sex differences in secondary BA concentrations, bacterial 7αDH activity led to higher tumour numbers in the colon of mice (figure 4f). Stratification according to tumour size revealed significance for small tumours, which suggests early-stage promotion of tumourigenesis by DCA rather than tumour progression.

Compared with *C. scindens*-colonised mice, *E. muris* was less abundant, which was linked to a more uniform distribution of the remaining bacterial species (figure 4c). DCA was detected in the caecum when 7αDH activity by *E. muris* was present and sex-specific differences (higher levels in females) were confirmed (figure 4e and online supplemental figure S5b). Several other secondary BAs were significantly elevated when *E. muris* 7αDH was present (eg, 12-oxo-chenodeoxycholic acid (CDCA), hyocholic acid, tauro-deoxycholic acid or lithocholic acid (LCA)). Interestingly, levels of the primary BA CA were higher in 7αDH- mice, indicating enhanced conversion in 7αDH+ mice. Similar to the effects of *C. scindens*, 7αDH activity by *E. muris* caused higher numbers of tumours in the colon, which was again linked primarily to small tumours (figure 4g).

To confirm the role of microbial DCA production in colonic tumour development, we performed gnotobiotic experiments in a murine model of spontaneous colitis-associated cancer driven by nAtf6 oncogene activation (nAtf6^{IEC})[20] combined with interleukin-10 knockout (*Il10*$^{-/-}$).[21] We used a different defined community of cultured gut bacteria, the OMM12, which lacks strains with 7αDH activity.[22] The addition of *E. muris* to OMM12 (OMM12+E) led to DCA production in the mouse gut (online supplemental figure S6a). Germ-free IEC-specific Atf6 transgenic mice deficient for IL-10 (nAtf6$^{IEC\ tg/wt}$; *Il10*$^{-/-}$) colonised with OMM12+E were characterised by more and earlier dropouts (online supplemental figure S7a). While the tumour incidence in nAtf6$^{IEC\ tg/wt}$;*Il10*$^{-/-}$ mice was similar in both colonisation groups (online supplemental figure S7b), *E. muris* significantly increased tumour numbers in the colon of these mice (online supplemental figure S7c,d), which was not the case in nAtf6$^{IEC\ fl/fl}$;*Il10*$^{-/-}$ mice. This suggests that both oncogene activation and DCA production are required in addition to inflammation in this model to drive colonic tumourigenesis.

To specifically demonstrate the role of bacterial 7αDH in promoting colon tumourigenesis, a wild-type strain of *Faecalicatena contorta* or its *baiH* mutant (Ω*baiH*), unable to produce dehydroxylated secondary BAs,[23] was used with BACOMI (without *C. scindens* and *E. muris*) to colonise germfree mice (online supplemental figure S1e). In contrast to wild-type *F. contorta*, the Ω*baiH* mutant strain was not able to produce DCA in colonised BACOMI mice (figure 5a and online supplemental figure S5c). After AOM/DSS treatment, the lack of DCA by Ω*baiH* induced fewer tumours in the colon than the wild-type strain of *F. contorta* (figure 5b). The presence of DCA resulted in higher numbers of small-sized tumours, confirming early-stage promotion of tumourigenesis (figure 5b). Treatment of human colon organoids with supernatants from wild-type *F. contorta* or the Ω*baiH* mutant strain incubated with CA led to higher numbers of Ki67+ epithelial cells when stimulated with the wild-type strain supernatant (figure 5c,d). Taken together, these results

Gut: first published as 10.1136/gutjnl-2024-332243 on 18 December 2025. Downloaded from http://gut.bmj.com/ on November 19, 2026 by guest. Protected by copyright, including for uses related to text and data mining, AI training, and similar technologies.

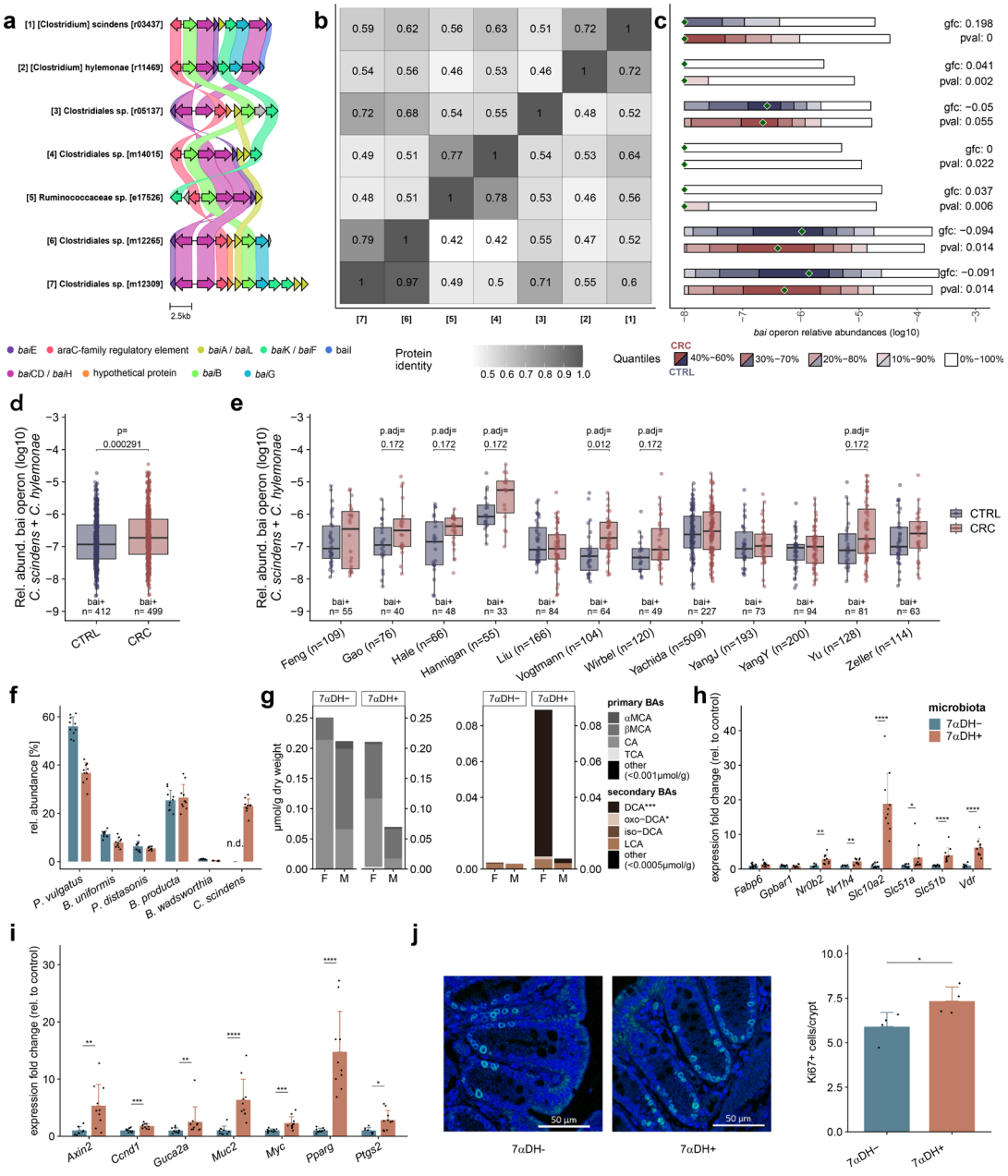


Figure 3 Identification of specific DCA-producing bacteria associated with CRC and functional evaluation in a gnotobiotic mouse model: (a) Genomic architecture of the *bai* operon in mOTUs (metagenomic operational taxonomic units) detected at >2% prevalence (n=2142). (b) Protein sequence identities between the different genomic architectures of the *bai* operon shown in (a). (c) Quantile plots of relative abundances of mOTU-specific *bai* operons over all CRC (n=1034) versus control (n=1108) samples. Due to high protein sequence similarity between *Clostridiales* sp. (m12265) and *Clostridiales* sp. (m12309) (last two bacteria listed), relative abundances are almost identical. (d) Cumulative relative abundance of the *bai* operons from *C. scindens* and *C. hylemonae* in samples from all cohorts. Only the samples with a detected *bai* operon from either of the two species are plotted. The corresponding number of positive samples is indicated above the x-axis. (e) Same as in d, but per study. The total number of samples is indicated below the x-axis. Studies that included <10 samples with detected *bai* operons in either of the groups (CTRL or CRC) were excluded. Adjusted p values <0.5 are shown (Wilcoxon rank-sum test with Benjamini-Hochberg adjustment, excluding samples without *bai* operon detected). (f) Relative abundances of bacterial species in colonic content of mice colonised with the BACOMI consortium with (7αDH+, n=10, 5F and 5M mice) or without (7αDH−, n=10, 5F/5M) *C. scindens* as measured by targeted qPCR. (g) Primary (grey) and secondary (brown) BA profile in caecal content quantified using LC-MS/MS (female and male mice are shown separately; the stacked bars indicate mean values; all individual concentrations are available in online supplemental table S4). (h, i) Expression of genes related to (h) BA metabolism and (i) epithelial cell proliferation and differentiation in the colonic mucosa. (j) Exemplary images of immunofluorescence staining for Ki67+ cells in colonic crypts of BACOMI 7αDH− or BACOMI 7αDH+) mice and corresponding quantification shown as bar plots (n=4 mice each). (f, h–j) Shown as mean values+SD. Statistics: Wilcoxon rank-sum test with Benjamini-Hochberg adjustment (*p.adj.≤0.05; **p.adj.≤0.01, ***p.adj.≤0.001, ****p.adj.≤0.0001). BA, bile acid; *bai*, BA inducible; BACOMI, BA-converting defined microbiota; CA, cholic acid; CRC, colorectal cancer; CTRL, control; DCA, deoxycholic acid; F, female; gfc, geometric fold change; Ki67, marker for cell proliferation; LCA, lithocholic acid; LC-MS/MS, liquid chromatography with tandem mass spectrometry; M, male; MCA, muricholic acid; p.adj., adjusted p value; pval, p value; qPCR, quantitative PCR; rel. abund., relative abundance; TCA, taurocholic acid; 7αDH, 7α-dehydroxylation.

Gut: first published as 10.1136/gutjnl-2024-332243 on 18 December 2025. Downloaded from http://gut.bmj.com/ on November 19, 2026 by guest. Protected by copyright, including for uses related to text and data mining, AI training, and similar technologies.

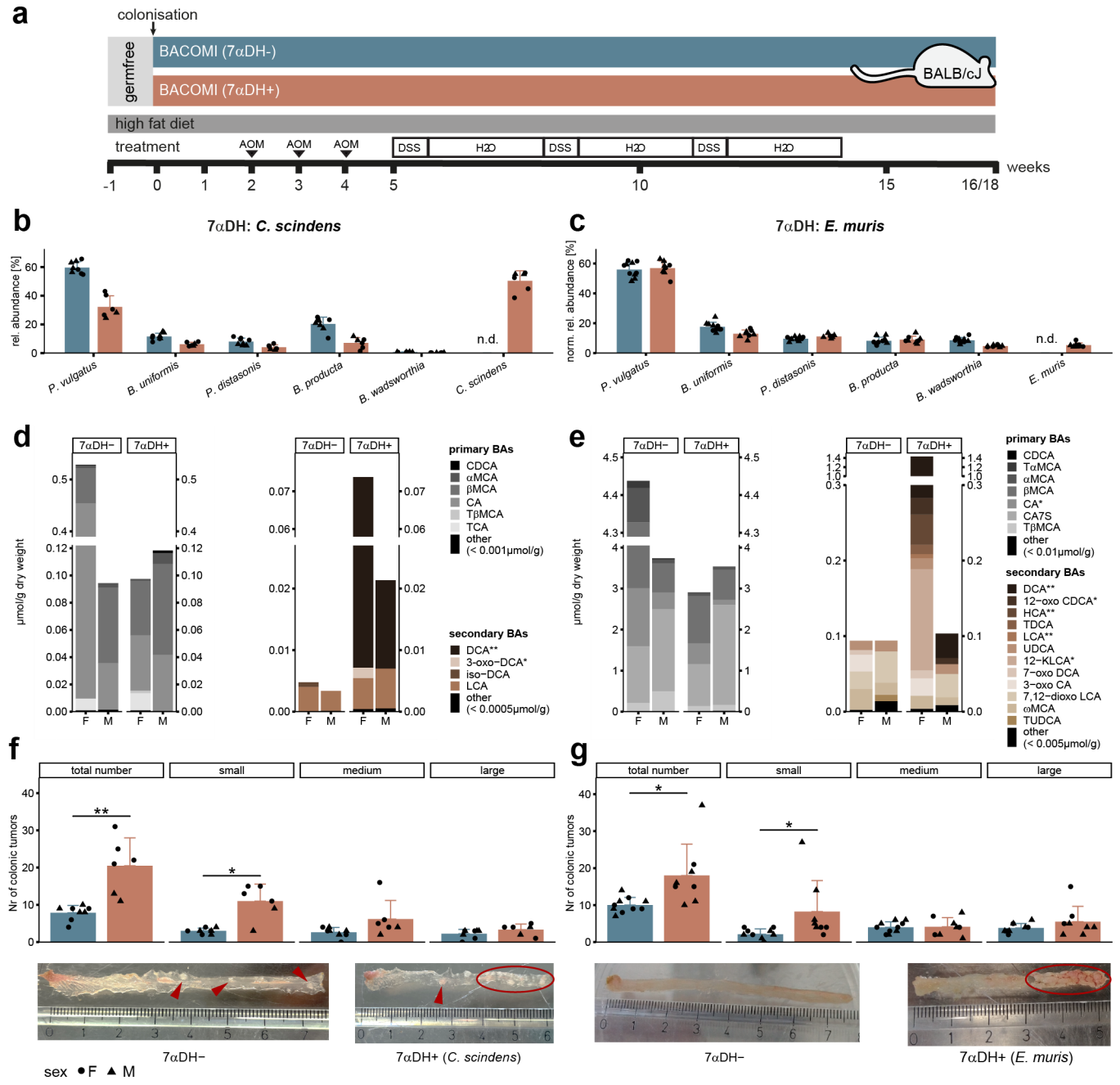


Figure 4 Effects of bacterial 7αDH on colonic tumourigenesis in gnotobiotic mice treated with AOM/DSS. (a) Setup of AOM/DSS experiments using BACOMI 7αDH− mice deprived of 7αDH activity and their BACOMI 7αDH+ counterparts colonised with either *C. scindens* (b, d, f, 7αDH−, n=8–7; 7αDH+, n=6) or *E. muris* (c, e, g, 7αDH−, n=10; 7αDH+, n=8). Mice were culled after either 16 weeks (*C. scindens*) or 18 weeks (*E. muris*). (b, c) Relative abundances of the bacterial species in colonic content as analysed by qPCR (b) or 16S rRNA gene amplicon analysis (c). (d, e) Primary (grey) and secondary (brown) BA profile in caecal content as quantified using LC-MS/MS (female and male mice shown separately). Data are shown as stacked bar plots of mean values. Individual concentrations are available in online supplemental table S4. (f, g) Number of colonic tumours; total or stratified according to their size: small (<1.2 mm^2), medium (1.2–2.5 mm^2), large (>2.5 mm^2). Exemplary macroscopic pictures of the colon are shown below the bar plots; single tumours or areas with many tumours are indicated with red arrowheads or circles. In (b, c, f, g) the sex of mice is indicated by different symbols (triangle=male; dots=female). Statistics (d–g): Wilcoxon rank-sum test with Benjamini-Hochberg adjustment (*p.adj.≤0.05; **p.adj.≤0.01, ***p.adj.≤0.001). AOM, azoxymethane; BACOMI, BA-converting defined microbiota; CA, cholic acid; CDCA, chenodeoxycholic acid; *C. scindens, Clostridium scindens;* DCA, deoxycholic acid; DSS, dextran sodium sulfate; *E. muris, Extibacter muris*; F, female; KLCA, keto-litocholic acid; LCA, lithocholic acid; LC-MS/MS, liquid chromatography with tandem mass spectrometry; M, male; MCA, muricholic acid; norm. rel., normalised relative; nr, number; qPCR, quantitative PCR; rel., relative; TCA, taurocholic acid; TUDCA, tauroursodeoxycholic acid; UDCA, ursodeoxycholic acid; 7αDH, 7α-dehydroxylation.

Gut: first published as 10.1136/gutjnl-2024-332243 on 18 December 2025. Downloaded from http://gut.bmj.com/ on November 19, 2026 by guest. Protected by copyright, including for uses related to text and data mining, AI training, and similar technologies.

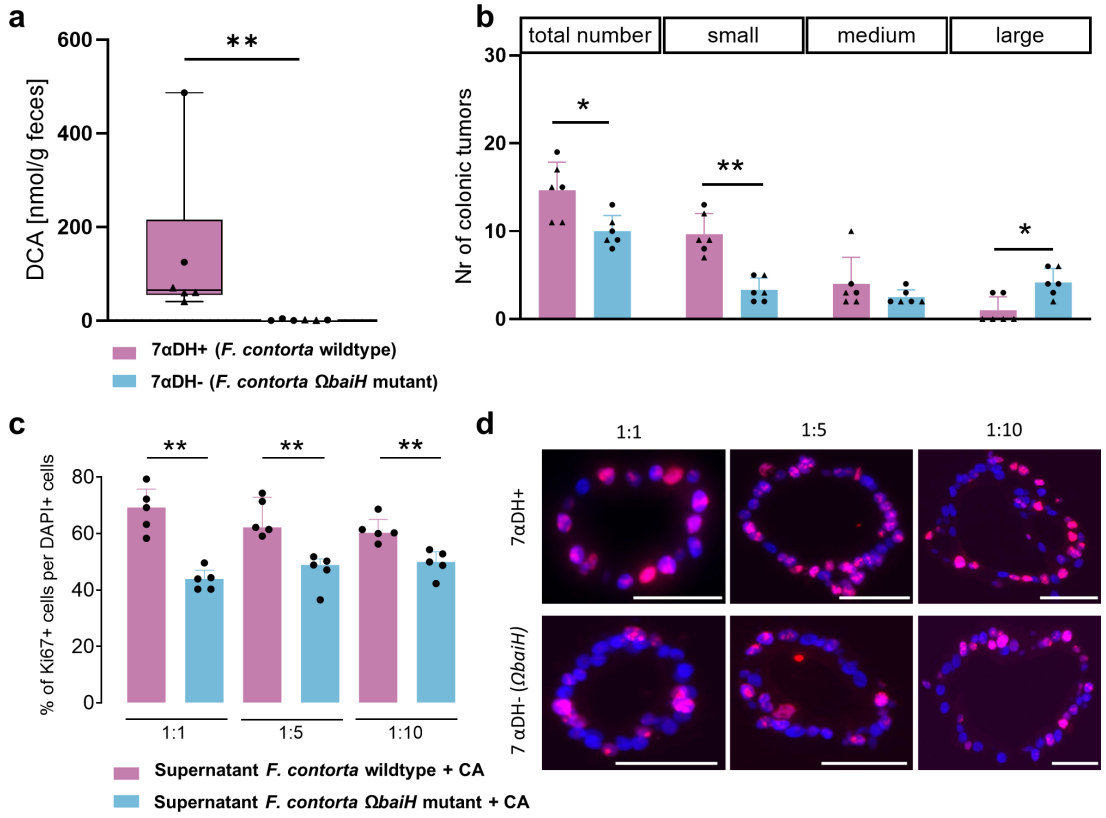


Figure 5 Causal role of bacterial 7αDH in epithelial cell proliferation and colonic tumourigenesis using a genetically modified strain in gnotobiotic mice and human colon organoids. (a) DCA concentrations in faeces of BACOMI mice colonised with *F. contorta* wild-type strain (7αDH+) or its Ω*baiH* mutant (7αDH–), as quantified by LC-MS/MS. Faeces was collected 1 week before the end of the experiment. The sex of mice (n=6 per colonisation group) is indicated by symbols: triangle, male; dots, female. (b) Number of colonic tumours; total or stratified according to their size: small (<1.2 mm^2), medium (1.2–2.5 mm^2), large (>2.5 mm^2). (c) Percentage of Ki67+ cells in human colonic organoids stimulated with different dilutions of cell-free bacterial supernatant from *F. contorta* wild-type versus Ω*baiH* mutant incubated with 100 µM CA for 24 hours (n=5). (d) Exemplary microscopic images of Ki67-staining from human organoids; scale bar=50 µm. Statistics: Wilcoxon rank-sum test (*p≤0.05; **p≤0.01). BA, bile acid; *bai*, BA inducible; BACOMI, BA-converting defined microbiota; CA, cholic acid; DAPI, 4',6-diamidino-2-phenylindole; DCA, deoxycholic acid; *F. contorta*, *Faecalicatena contorta*; Ki67, marker for cell proliferation; LC-MS/MS, liquid chromatography with tandem mass spectrometry; nr, number; 7αDH, 7α-dehydroxylation.

demonstrate the causal role of bacterial 7αDH in promoting colonic epithelial cell proliferation and tumourigenesis.

DISCUSSION

This study demonstrates the role of secondary BAs produced via gut bacterial 7αDH as tumour-promoting metabolites in experimental CRC. In contrast to non-physiological DCA supplementation in previous studies, we provide causal evidence linking the CRC risk-promoting effects of Western diets to functional adaptation of the gut microbiota. The experiments in $APC^{1311/+}$ pigs substantiate the clinical relevance of Western diet-mediated stimulation of microbial BA metabolism and suggest that promoting the excretion of BAs is a therapeutic option to limit their tumourigenic effects in the large intestine.

Bacterial 7αDH activity from the specific DCA-producers *C. scindens*, *E. muris* and *F. contorta* enhanced colonic tumourigenesis in gnotobiotic mice. This validates our own findings about the higher occurrence of *bai* operons from *C. scindens* and *C. hylemonae* in metagenomes from patients with CRC and is an important experimental proof of previous observational data on higher numbers of 7αDH+ bacteria in faeces of patients with CRC or individuals at high CRC risk.[5–7] It also provides physiologically relevant evidence for the tumour-promoting effects of secondary BAs in murine CRC models compared with previously tested oral DCA supplementation and observed effects in the small intestine.[9–12] Of note, 7αDH caused significantly higher numbers of small but not large colonic tumours in our gnotobiotic mouse experiments with AOM/DSS treatment. This may indicate that DCA promotes cellular processes underlying tumour initiation rather than progression in the colonic epithelium of susceptible hosts. Data obtained in the $nAtf6^{IECtg/wt}$; $Il10^{-/-}$ gnotobiotic model of CRC demonstrates the importance of host genetic modification besides gut inflammation for the tumour-promoting effect of 7αDH+ bacteria.

There are multiple possible mechanisms for the tumour-promoting effect of DCA. For instance, it was shown to stimulate cancer stemness in colonic epithelial cells by modulating β-catenin signalling.[24] It also triggered proliferation and DNA damage in $Apc^{Min/+}$ Lgr5+ intestinal stem cells by antagonising the BA receptor farnesoid X receptor.[25] Moreover, oral administration of DCA and HFD-associated secondary BAs promoted proliferation of Lgr5+ stem cells via the BA receptor Takeda G protein-coupled receptor 5 (TGR5).[26] Consistently, 7αDH-mediated production of DCA did not induce colonic tumours without AOM/DSS in our study but it increased Ki67+

Gut: first published as 10.1136/gutjnl-2024-332243 on 18 December 2025. Downloaded from http://gut.bmj.com/ on November 19, 2026 by guest. Protected by copyright, including for uses related to text and data mining, AI training, and similar technologies.

epithelial cell numbers and enhanced the expression of genes previously shown to be involved in secondary BA-associated colonic tumourigenesis.[24 25] The tumour-promoting role of secondary BAs in susceptible hosts due to diet is also supported by our observation of Western diet-driven increase in Ki67+cells in the colon of *APC*$^{1311/+}$ pigs. Furthermore, enhanced faecal excretion of BAs by COL was associated with reduced proliferation in the colonic epithelium. This finding provides additional preclinical evidence for the potential use of COL for CRC prevention. Previous data in mice showed that COL decreased the expression of genes involved in epithelial cell proliferation in the colon and that it could prevent streptozotocin and HFD-induced hepatocellular carcinoma.[27] The use of BA sequestrants in individuals at increased CRC risk appears to be promising for prevention, since prediagnostic high plasma levels of BAs were linked to CRC outcome in a prospective study.[28] In this context of preventive BA reduction, it is worth noticing that secondary BAs also increased the expression of genes with essential regulatory functions (eg, *Guca2a*, *Muc2*, *Pparg*) in our gnotobiotic mice, suggesting that 7αDH-associated microbial metabolites have a fundamental role in regulating intestinal epithelium homeostasis and regeneration. Thus, low but not completely abolished DCA levels seem to be a promising preventive or therapeutic target for CRC risk reduction. Recently, BAs were shown to be required for TGR5-dependent regeneration of intestinal epithelial cells and protection from colitis in mice,[26] further supporting the importance of physiological BA levels.

In the mouse experiments, we detected a larger caecal BA pool and higher DCA concentrations in female compared with male animals. It is known that female and male mice differ in their BA composition and female mice tend to have higher serum and liver DCA concentrations.[29] Moreover, sex hormones influence hepatic BA metabolism, including their production, secretion and absorption.[29] Therefore, our data is in line with already described sex differences in BAs and illustrates the importance to investigate both sexes. Besides BAs, sex hormones also affect CRC risk directly: testosterone increases CRC risk,[30] while oestrogen has the opposite effect.[31] This possibly explains why, in our gnotobiotic experiments, colonic tumour numbers were increased by secondary BA production in both male and female mice despite markedly higher DCA concentrations in the latter group.

Besides the causal role of secondary BAs in experimental CRC as demonstrated here, Western diet may promote CRC risk via the microbiome in several manners. For example, a recent study by Yang *et al*[32] demonstrated that experimental CRC was associated with higher levels of *Alistipes* spp and dysregulation of gut microbial co-metabolism leading to higher levels of glycerophospholipids. Moreover, diets high in fat content are usually associated with increased occurrence of *Enterobacteriaceae*, potentially including *pks*+ *Escherichia* coli with tumourigenic effects.[33] CRC risk does not exclusively arise from the increase in tumour-promoting factors but also from the lack of tumour-suppressive dietary compounds, including complex carbohydrates fermented by gut bacteria to short chain fatty acids such as butyrate.[4 5] Furthermore, Western or HFDs are very diverse in terms of fat content and quality, with consequences regarding effects on the host. Recent studies showed that a ketogenic diet, highly enriched in fat and very low in carbohydrates, reduced experimental colonic tumourigenesis.[34] However, the long-term clinical relevance of ketogenic diets remains to be demonstrated. Taken together, these findings highlight the complexity of diet-associated changes in gut microbial metabolism and support the use of model organisms and experimental diets with detailed composition to unravel the influence of nutrition on CRC development or prevention.

In conclusion, our studies demonstrate the causal role of gut microbial 7αDH activity in experimental CRC. Secondary BAs, in particular DCA, are implicated in the tumour-promoting effects of Western diets, which provides a promising target for CRC prevention via dietary intervention or modulation of gut microbial BA metabolism.

METHODS

Animal work

All experiments were carried out according to the German Animal Welfare Act and the European Union Normative for Care and Use of Experimental Animals. Individual approval numbers from the corresponding authorities are provided in the following subsections that describe the specific experiments.

Porcine experiments

These experiments were approved by the Federal Government of Bavaria (permit no. ROB55.2-2-2532.Vet_02-18-33). Pigs were provided by the Chair of Livestock Biotechnology at the Technical University of Munich, Germany, and were housed and sampled at the animal facility Thalhausen (Faculty of Life Science Weihenstephan, Freising, Germany).

Dietary Interventions in *APC*$^{1311/+}$ pigs

The experimental design is depicted in online supplemental figure S1a. *APC*$^{1311/+}$ pigs (German landrace×minipig crossbreed)[13] underwent colonoscopy at the age of 3 months to enable their separation into two groups with a comparable distribution of individuals in terms of polyp numbers and size, sex and littermates. Both groups were fed a standard diet until the dietary intervention started at the age of 4 months to allow for recovery after colonoscopy. The CTRL and experimental diet enriched in RL were specifically designed for this experiment and purchased from ssniff Spezialdiäten GmbH (Soest, Germany; cat. no. S5745-S074 and S5745-S076, respectively). Main differences between the diets are illustrated in online supplemental figure S1a and their detailed compositions are provided in online supplemental table S1. The diets were fed to the pigs in a restricted manner (approximately 1 kg/day) for 3 months until the age of 7 months. At the end of the feeding period, faecal samples were taken, and colonoscopy was performed, including biopsy collection. Two RL pigs dropped out of the study due to tumour-independent reasons (meningitis and a foot malformation).

For the second feeding trial testing the effects of COL, the overall experimental design was as in the first experiment (online supplemental figure S1b). However, *APC*$^{1311/+}$ pigs were assigned to three groups instead of two (n=4–5 pigs each): CTRL, RL and COL (=RL diet supplemented with 12 g/kg COL; Ratiopharm GmbH, Ulm, Germany; EAN 4150037520609). The recommended dose by the manufacturer is 4–16 g/day for adult subjects. Additional components of the drug COL besides the active agent were added to CTRL and RL diet. Detailed diet compositions are available in online supplemental table S1.

Colonoscopy

Pigs underwent colonoscopy 1 month prior to dietary intervention and after the 3 months of experimental feeding. To reduce the load of faecal material in the large bowel, pigs were fasted for 24 hours before the procedure. Based on bodyweight, pigs were narcotised (0.2 mg/kg ketamine and 0.05 mL/kg azaperone) and the large bowel was flushed with tap water to remove

Gut: first published as 10.1136/gutjnl-2024-332243 on 18 December 2025. Downloaded from http://gut.bmj.com/ on November 19, 2026 by guest. Protected by copyright, including for uses related to text and data mining, AI training, and similar technologies.

remaining luminal content. Tissue biopsies and images were taken using a STORZ colonoscopy system (Flexible SILVER SCOPE). To ensure accuracy and reproducibility, each colonoscopy video was independently reviewed twice for verification of total polyp number and morphological classification within the evaluated 40 cm segment of the colon. During each procedure, a minimum of five representative polyps per pig were obtained by endoscopic biopsy for histopathological assessment. Regressive polyps were characterised by elevated polypoid morphology with a white surface layer and partial tissue apoptosis. In contrast, progressing polyps predominantly exhibited sessile or pedunculated morphologies. Most progressing polyps were sessile, featuring a flat, broad base and a reddish superficial layer, hallmarks of actively growing polyps.

Collection of faeces and sampling

In both pig trials, fresh faecal samples were collected prior to (4 months of age) and immediately after dietary intervention (7 months of age) before colonoscopy. In brief, faecal material was taken directly from the rectum of each pig using sterile gloves and placed into individual, sterile plastic containers. Solely the material from core areas of the faeces was collected using a sterile spatula. Samples were immediately frozen on dry ice and stored at −80°C for later sequencing and metabolomics. Tissue samples from the rectum were collected either during colonoscopy (pig trial 1) or after the pigs were culled (pig trial 2). The resulting samples were formalin-fixed and paraffin-embedded tissue blocks that were stored at room temperature.

Mouse experiments

BACOMI consortium

The defined microbial community BACOMI (Bile acid-converting microbiota) contains six bacterial species (all obtained from the Leibniz-Institute DSMZ - German Collection of Microorganisms and Cell Cultures, Braunschweig, Germany) that can transform the host-derived primary BAs into dehydroxylated secondary BAs (adapted from Ridlon *et al*)[35] (online supplemental figure S1c). *Bacteroides uniformis* (*B. uniformis*) DSM 6597, *Phocaeicola vulgatus* (*P. vulgatus*) DSM 1447 and *Parabacteroides distasonis* (*P. distasonis*) DSM 20701 express bile salt hydrolases (BSH) that produce free primary BAs from conjugated counterparts. *Bilophila wadsworthia* (*B. wadsworthia*) DSM 11045 can further metabolise taurine released by BSH activity into H_2S. *Clostridium scindens* (*C. scindens*) DSM 5676 is the key member of the BACOMI consortium, as it is the only species with 7α-dehydroxylating (7αDH) activity. Finally, *Blautia producta* (*B. producta*) DSM 2950 was added due to being a dominant human gut bacterium that is H_2-consuming, acetogenic, able to isomerise bile acids and thus increases variability of the BA pool. The other 7αDH+ species *Extibacter muris* (*E. muris*) DSM 28560 was isolated and described by us previously.[36 37] *Faecalicatena contorta* S122 was previously isolated and genetically modified to create a Ω*baiH* mutant strain unable to produce DCA.[23] All bacteria except for *B. wadsworthia* were cultured in brain heart infusion medium supplemented with resazurin, hemin, yeast extract and L-cysteine under anaerobic conditions. *B. wadsworthia* was cultured as previously described.[38]

OMM12 ± *E. muris* consortium

OMM12 is a defined community of cultured bacteria representing the five major phyla in the mouse gut.[22] We amended this consortium by the addition of the 7αDH+ species *E. muris* DSM 28560. For the generation of cryo-stocks, individual strains were grown in anaerobic Akkermansia medium. Strains were mixed equally (based on OD measurements) and mixed with 20% glycerol in a 1:1 ratio (exact mixing volumes and strain designations are given in online supplemental table S7).

Gnotobiotic mouse experiments

The experiments in AOM/DSS treated mice were approved by the Ministry of Social Affairs, Health, Integration and Consumer Protection of the state Brandenburg (permit no. 2347-15-2021). Germ-free male and female wild-type mice (BALB/cJ) were kept in positive-pressure isolators at the animal facility of the German Institute for Human Nutrition Potsdam-Rehbruecke (Nuthetal, Germany) with a 12 hours light-dark cycle at 22±2°C and 55±5% air humidity. Starting 1 week prior to colonisation, the mice were switched from standard diet to a HFD (online supplemental table S1). Mice (n=8–10 per group) were colonised by gavage (10^8 cells per bacterium in 100 µL medium; 50 µL orally and 50 µL rectally at day 0 and 2) with BACOMI either with (7αDH+) or without (7αDH−) *C. scindens*. After colonisation, mice were either kept for 12 weeks (online supplemental figure S1d and figure 3) or subjected to further treatment to induce experimental CRC (figure 4). In the latter case, mice received three intraperitoneal injections of AOM (Merck, Darmstadt, Germany) (5 mg/kg body weight) in the interval of 1 week, starting at week 2 after colonisation. 5 days after the final AOM injection, mice were treated with three cycles of DSS (MP Biomedicals, Santa Ana, USA) with 5 days of DSS (1.5% in drinking water) followed by 16 days of normal drinking water. Mice were culled 2 weeks after the end of the AOM/DSS treatment and colonic tumours were counted using a binocular microscope. The colonisation and AOM/DSS treatment of mice with *E. muris* and *F. contorta* (wild-type or Ω*baiH* mutant) followed the same protocol, but mice colonised with *E. muris* were kept 2 weeks longer after colonisation and prior to AOM/DSS treatment to confirm colonisation status, and the mice colonised with the *F. contorta* strains received two cycles of DSS (online supplemental figure S1e). For BACOMI with *C. scindens* colonisation, three mice (male n=1, female n=2) dropped out in the 7αDH+ group during the first DSS cycle, whereas for the 7αDH− group, two mice (male n=1, female n=1) dropped out at the end of the third DSS cycle or after the first AOM injection, respectively. For BACOMI with *E. muris* colonisation, two female mice dropped out in the 7αDH+ group after the first DSS cycle. For BACOMI with wild-type *F. contorta*, one female mouse dropped out in the first DSS cycle and a male mouse dropped out in the second DSS cycle. For BACOMI with the mutant *F. contorta* strain (Ω*baiH*), two male mice dropped out in the first DSS cycle.

Germ-free IEC-specific expression of activated (p50) nAtf6 transgenic mice ($nAtf6^{IEC}$)[20] was crossed to germ-free $Il10^{-/-}$ mice. Heterozygous mice with monoallelic nAtf6 expression ($nAtf6^{fl/wt}$; $Vil\text{-}Cre^{tg/wt}$; $Il10^{-/-}$) and floxed controls ($nAtf6^{fl/wt}$; $Vil\text{-}Cre^{wt/wt}$; $Il10^{-/-}$) were used for gnotobiotic work.[21] These experiments were approved by the Committee on Animal Health Care and Use of the State of Upper Bavaria (Regierung von Oberbayern; AZ TVA 55.2–2532.Vet_02-18-121). 4-week-old mice were inoculated orally (50 µL) and rectally (100 µL) with cryo-stocks of the OMM12 or OMM12+*E. muris* (OMM12+E) strain mixture at day 0 and day 3, received a standard diet (autoclaved V1124-300, Ssniff, Soest, Germany) ad libitum and kept colonised for 12 weeks. All mice were euthanised with CO_2 at the end of an experiment (age 16 weeks) or when abortion criteria were met.

Gut: first published as 10.1136/gutjnl-2024-332243 on 18 December 2025. Downloaded from http://gut.bmj.com/ on November 19, 2026 by guest. Protected by copyright, including for uses related to text and data mining, AI training, and similar technologies.

Quantitative real-time PCR for intestinal gene expression

The Dynabeads mRNA purification kit (Thermo Fisher Scientific, Waltham, USA) was used for mRNA isolation. Lysis buffer (200 μL) and 10 zirconium beads were added to approximately 5 mg of intestinal tissue stored at −80°C in RNA later tissue reagent (Qiagen, Venlo, Netherlands). A tissue lyser (Qiagen, Hilden, Germany) was then used for homogenisation (2×2 min at 50 Hz with a 2 min break in between). The lysate was pulled through a syringe five times with a 1 mL syringe and centrifuged (18 800x g, 2 min, room temperature). The rest of the protocol was as per the manufacturer's instructions. mRNA concentrations were determined using a Nanodrop (Peqlab VWR, Radnor, USA) and 20 ng were used for reverse transcription using the RevertAid H Minus First Strand cDNA Synthesis kit (Thermo Fisher Scientific) according to manufacturer's recommendations. For qPCR, the mastermix was prepared according to the manufacturer's recommendations given by the Quantinova SYBR Green PCR Kit (Qiagen, Hilden, Germany), and forward and reverse primers added (0.5 μM each) (online supplemental table S5). Then, 4 ng template cDNA was used in a total reaction volume of 10 μL. Samples were amplified using the 7500 Fast Real-Time PCR System (Applied Biosystems, Waltham, USA). To determine C_T-values, the Life Technologies 7500 Software (V.2.3) was used. Normalisation was to the housekeeping gene *Rpl13a,* which encodes for the 60S ribosomal protein L13a. Results were calculated relative to the control group of 7αDH− mice.

Immunohistochemistry and immunofluorescence

Specimens from the two pig trials were fixed in 4% formaldehyde solution for 24 hours, embedded and sectioned (3 μm). The tissue sections were then deparaffinised, antigen unmasked (citrate buffer, pH=6) and endogenous peroxidases were inactivated in 3% H_2O_2 for 10 min. After blocking for 1 hour (2% goat serum in phosphate buffered saline (PBS)), sections were incubated overnight at 4°C with the primary antibody for Ki67 (Rabbit, DSC innovative Diagnostik-System, Hamburg, Germany, KI681C002, dilution 1:400) followed by a second overnight incubation with the secondary antibody (Goat Anti-Rabbit IgG, Santa Cruz, Dallas, USA, sc-2780, dilution 1:400). Peroxidase activity was detected using diaminobenzidine substrate or the VECTASTAIN Elite ABC Kit (Vectorlab, Newark, USA, PK-6100), respectively. Staining of Ki67 was considered positive and quantified only when detected in nuclei. Ten randomly selected fields (magnification ×40) from each tissue section were analysed. Values are presented as the percentage of the stained cells per area.

For the gnotobiotic mouse trial (figure 3), the dissected tissues were fixed using Methacarn solution and embedded in paraffin. Tissues were cut into 4 μm-thick sections and deparaffinised by heating (60°C, 15 min) followed by two times xylol for 3 min. The specimens were then rehydrated using a decreasing alcohol series: 100% for 2 min, 96% for 2 min, and 70% for 1 min, followed by water for 1 min. After rinsing twice in water (5 min each), the specimens were boiled in 10 mM citrate buffer (pH=6) for 30 min for antigen retrieval, followed by 30 min of cooling. Thereafter, the specimens were washed three times with water for 5 min, once with PBS for 5 min, and then blocked with PBS containing 5% goat serum for 1 hour at room temperature. Primary antibodies against Ki67 (abcam, Cambridge, UK, ab15580, dilution 1:200) were incubated overnight at 4°C. Specimens were then washed three times in PBS (5 min each) and incubated with the secondary antibody (AlexaFluor-488, Thermo Fisher Scientific; dilution 1:200), and Hoechst (Merck, Darmstadt, Germany; dilution 1:200) for 1–2 hours at room temperature. All antibodies were diluted in PBS containing 1% bovine serum albumin and 0.3% Triton X-100. Finally, the specimens were washed in PBS for 5 min each and covered with glass slides using mounting medium (Vector Laboratories, Newark, USA). For imaging, a confocal laser microscope was used (LSM 780 microscope, Zeiss, Oberkochen, Germany). Tile scans with 40× magnification were acquired and analysed with the ZEN (black edition) V.2.3 software (Zeiss).

Microbiota composition analysis

Metagenomic DNA was obtained using a modified version of a previously published protocol.[39] Cells were lysed mechanically via bead-beating and DNA was purified on columns (Macherey-Nagel, Düren, Germany). A robotised platform (Biomek4000, Beckman-Coulter, Aachen, Germany) was then used for library construction. The V3-V4 regions of 16S rRNA genes were amplified (25 cycles) in a two-step PCR using primers 341F (5′-cctacgggnggcwgcag) and 785R (5′-gactachvgggtatctaatcc)[40] and 24 ng of template DNA. A double combinatorial indexing strategy was used. Amplicons were purified using the AMPure XP system (Beckmann Coulter), pooled in equimolar amounts and sequenced in paired-end mode using a MiSeq system (Illumina, San Diego, USA).

Raw data were processed using IMNGS (https://www.imngs.org),[41] an online platform based on UPARSE.[42] Sequences were clustered into operational taxonomic units (OTUs) at 97% sequence similarity and only those with a relative abundance ≥0.25% in at least one sample were kept to exclude spurious OTUs.[43] Parameters for data processing were: min/max sequence length, 300–500 nt; barcode mismatch, 1; end-trim length, 15; max. no. expected errors, 3; trimming q score, 3. The number of sequences per sample after filtering was 26 286±8044 for the first pig trial and 12 564±3954 for the gnotobiotic mouse experiment with *E. muris*. Downstream diversity and composition analyses were performed in Rhea (https://github.com/Lagkouvardos/Rhea).[44] For the first pig trial, taxonomies were assigned using SILVA release 128. Several families showed a significantly different behaviour between the feeding groups over time. A pseudocount (lowest value×10) was added to the normalised relative abundance of each family per sample before calculation to avoid division by zero. For family comparison over time, a start-adjusted delta value was calculated as follows: (end – start) / start. For changes in α-diversity, original values without pseudocount were used for the same calculation. Identities of the OTUs for the gnotobiotic mouse experiment were confirmed using Eztaxon.[45] Normalised relative abundances are plotted in figures 1 and 4 and provided in online supplemental tables S2 and S4.

For the gnotobiotic mouse trials with *C. scindens,* the QIAmp Fast DNA Stool Mini Kit (Qiagen, Hilden, Germany) was used to extract and purify DNA from colon content. Approximately 50–80 mg frozen content was added to a cryotube containing ca. 100 mg of 0.1 mm glass beads, and 1 mL of InhibitEx buffer, followed by bead-beating (Uniprep, UniEquip, Neuried, Germany) for 2×5 min at 3000 rpm. All samples were processed according to the manufacturer's instructions except for the elution volume (changed to 70 μL). For DNA isolation from bacterial cultures, the Genomic DNA from Microorganisms Kit (Macherey-Nagel) was used as per the manufacturer's instructions. The disruption time was 12 min, and the samples were eluted twice using the same elution buffer.

Gut: first published as 10.1136/gutjnl-2024-332243 on 18 December 2025. Downloaded from http://gut.bmj.com/ on November 19, 2026 by guest. Protected by copyright, including for uses related to text and data mining, AI training, and similar technologies.

A standard curve plotting bacterial cell number against C_T-value was established for each BACOMI species using real-time qPCR and species-specific primers (online supplemental table S5). The standard curve was generated from overnight bacterial cultures and cell numbers were determined using a Thoma cell counting chamber (Fein-Optik, Herburg, Germany). For quantification, bacterial DNA was isolated from colon content and bacterial cell numbers (online supplemental table S4) were calculated using the generated standard curve.

Analysis of *bai* operon occurrence in metagenomes

To quantify the occurrence of *bai* operons in faecal metagenomes, we first extracted *bai* sequences from Kim *et al*[46] and retained the operons harbouring at least seven of the eight genes found in experimentally validated *bai* operons. The complete contig of each *bai* sequence was downloaded from GenBank. GECCO (V.0.9.7) was trained on the complete contigs with default parameters using Pfam V.35.0[47] and *bai*-specific HMMs[7] as training features. We then ran GECCO on ProGenomes3 (PG3) representative genomes (n=41 171) and selected those clusters with more than seven unique *bai* genes, since all experimentally verified *bai* operons had >7 unique *bai* genes with our approach, based on *bai* genes HMM annotation. This resulted in a total of 18 PG3 genomes with complete *bai* operons and we extracted the protein sequence of each of the individual operons. We then computed protein sequence similarity across the *bai* genes between operons from all genomes to understand how divergent the sequences are, which is important to know prior to quantifying relative abundances in metagenomes. Protein sequence similarity was computed by pairwise alignment (global mode, BLOSUM62 substitution matrix) as implemented in Biopython V.1.81.[48] Next, we used mmseqs map (V.13.45111) to map protein sequences of the complete operons of all 18 clusters against our reduced GMGC (Global Microbial Gene Catalogue) gut catalogue (n=13 788 251 ORFs) to identify which genes contained parts of the operons. This approach also enabled species-resolved *bai* operon quantification. We then collected a total of n=2142 samples from case-control metagenomic studies of CRC (n=1034 CRC, n=1108 CTRL, see online supplemental table S8 for an overview). These metagenomes were processed and profiled as follows: (1) Raw reads were cleaned using bbduk (V.38.93), including low-quality trimming on either side (qtrim=rl trimq=3), discarding low-quality reads (maq=25), adapter removal (ktrim=r k=23 mink=11 hdist=1 tpe=true tbo=true; against the bbduk adapter library), and length filtering (ml=45); (2) Reads were screened for host contamination using kraken2 (V.2.1.2) against the human hg38 reference genome with ribosomal sequences masked (Silva_v_138); (3) Cleaned reads were then mapped onto our reduced human gut gene catalogue using BWA-MEM (V.0.7.17) with default parameters and alignments were filtered to >45 bp alignment length and >97% sequence identity. Reads aligning to multiple genes contributed fractional counts towards each hit gene. Alignment counts for a gene were normalised against its length, then scaled up according to the strategy employed by NGLess (https://ngless.embl.de/Functions.html#count) and propagated to the functional features with which the gene is annotated. Extensive use of gffquant (V.2.10.0, https://github.com/cschu/gff_quantifier) was made throughout the functional profiling workflow. As information about which individual GMGC gene corresponded to a part of the *bai* operon of a given bacterial species was available, we obtained species-resolved relative abundances of *bai* operons. Values for all GMGC genes belonging to a specific species' *bai* operon were summed to compute total relative abundance for the *bai* operon of the given bacterial species. We only included *bai*-encoding species if they occurred at a prevalence of at least 2% in the entire dataset. To calculate the prevalence of the bacterial species, we performed taxonomic profiling using mOTUs (V.3.1) with default parameters after having run the bbduk quality filtering as described above. Differential abundance analysis was performed using a linear mixed model with the study as a random effect, through the SIAMCAT package. A pseudocount of 1e-8 was used for plotting zero values on a logarithmic scale (figure 3c). For figure 3d,e, zero values of the two respective mOTUs were not considered. For figure 3e, only studies with more than 10 samples containing *bai* operons of either *C. hylemonae* or *C. scindens* in each group were included.

Bile acid measurements

Pig stool samples from trial 1 and 2 were analysed as described previously by Wegner *et al* and Reiter *et al*, respectively.[49 50]

For the BACOMI mouse experiments, about 30 mg of lyophilised caecal content (experiments with *C. scindens*) or 60 mg faeces (experiments with *F. contorta*) were mixed with 450 μL acetonitrile, followed by 15 min vortexing and then centrifugation (13 000×g, 60 min, 21°C). Supernatant (300 μL) was mixed with the internal standards (ISTDs) d_4-CDCA and d_4-LCA (10 μM each) and dried in a SpeedVac system (Jouan RC10.22, Thermo Fisher Scientific). The residue was dissolved with methanol and water (1:1). Chromatographic separation of 5 μL sample was achieved on a 1290 Infinity II HPLC (Agilent Technologies) equipped with a Poroshell EC-C18 column (Agilent Technologies; 3.0×150 mm, 2.7 μm) connected to a guard column (3.0×5 mm, 2.7 μm) of the same material. The column was tempered to 30°C. A mobile phase system consisting of 10 mM ammonium acetate/acetonitrile (80:20 v:v; solvent A) and water/acetonitrile (20:80 v:v; solvent B) was applied at a flow rate of 0.2 mL/min. The initial solvent composition of 85% solvent A was maintained for 6 min. Then, solvent A was decreased stepwise to 70, 40 and 20% within 20, 30 and 40 min of total run-time, respectively. After 45 min, the mobile phase reached initial conditions again. MS/MS analysis was carried out using a 6495C triple-quadrupole mass spectrometer (Agilent Technologies) operating in the negative electrospray ionisation mode (ESI−). The ion source parameters were: sheath gas temperature, 400 °C; sheath gas flow, 12 L/min of nitrogen; nebuliser pressure, 40 psi; drying gas temperature, 120 °C; drying gas flow, 15 L/min of nitrogen; capillary voltage, 4500 V; nozzle voltage, 0 V; iFunnel high pressure RF voltage, 90 V and iFunnel low pressure RF voltage, 60 V. A total of 30 compounds (28 bile acids and 2 ISTDs) were simultaneously analysed by single reaction monitoring or, if feasible, by multiple reaction monitoring. High-performance liquid chromatography-tandem mass spectrometry (HPLC-MS/MS) parameters are given in online supplemental table S6. Quantification was performed using MassHunter Workstation Quantitative Analysis for QQQ (V.10.1; Agilent Technologies). Analytes were externally calibrated in the concentration range of 0.09–90 μM (ISTDs constantly 10 μM). BA concentrations were normalised to dry weight of the caecal content subjected to extraction.

For the gnotobiotic mouse experiment with *E. muris*, samples were lyophilised overnight at −60°C. The dried caecal contents were weighed, and six ceramic beads (2.5 mm) were added to each tube. Proportionally to the weight of each sample, between 500 μL and 1500 μL of MeOH/H_2O (2/1) + 0.1% formic acid was used as extraction solvent. Samples were homogenised in a

Gut: first published as 10.1136/gutjnl-2024-332243 on 18 December 2025. Downloaded from http://gut.bmj.com/ on November 19, 2026 by guest. Protected by copyright, including for uses related to text and data mining, AI training, and similar technologies.

Precellys 24 Tissue Homogenizer (Bertin Instruments, Montigny-le-Bretonneux, France) at 6500 rpm 2×20" beat and 20" rest. The homogenised caecal samples were centrifuged at 21 000 rcf for 15 min at 4°C. 100 uL from each supernatant or calibration standard was transferred into individual wells of 2 mL 96-well plate. 50 μL of an ISTD solution (CA-d_4, CDCA-d_4, TCA-d_4, TUDCA-d_4, DCA-d_4 and LCA-d_4, each at 2 μM in methanol) was pipetted in each well. Immediately after the addition of ISTD, 600 μL of 0.2% formic acid in H_2O was added to each sample or calibration standard level. The 96-well plate was shaken with an orbital shaker at 300 rpm and centrifuged at 2000x g, 5 min, 4°C. The contents of the 96-well plate were extracted by solid phase extraction with an Oasis HLB 96-well uElution plate (Waters, Milford, USA). The extracted samples were dried in a Biotage SPE Dry 96 (Biotage, Uppsala, Sweden) at 20°C and reconstituted with 100 μL of MeOH/H_2O (50/50). The plate was shaken with an orbital shaker at 300 rpm, 5 min and centrifuged at 2000x g, 5 min, 4°C. The samples were injected on the liquid chromatography-high resolution mass spectrometry (LC-HRMS) system.

The quantitative method was performed on an Agilent ultrahigh-performance liquid chromatography 1290 series coupled in tandem to an Agilent 6530 Accurate-Mass Q-TOF mass spectrometer.[51] The separation was done on a Zorbax Eclipse Plus C18 column (2.1×100 mm, 1.8 μm) and a guard column Zorbax Eclipse Plus C18 (2.1×5 mm, 1.8 µm) (both Agilent Technologies). The column compartment was kept heated at 50°C. Two different solutions were used as eluents: ammonium acetate (5 mM) in water as mobile phase A and pure acetonitrile as mobile phase B. A constant flow of 0.4 mL/min was maintained over 26 min of run time with the following gradient (expressed in eluent B percentage): 0–5.5 min, constant 21.5% B; 5.5–6 min, 21.5–24.5% B; 6–10 min, 24.5–25% B; 10–10.5 min, 25–29% B; 10.5–14.5 min, isocratic 29% B; 14.5–15 min, 29–40% B; 15–18 min, 40–45% B; 18–20.5 min, 45–95% B; 20.5–23 min, constant 95% B; 23–23.1 min, 95–21.5% B; 23.10–26 min, isocratic 21.50% B. The system equilibration was implemented at the end of the gradient for 3 min in initial conditions. The autosampler temperature was maintained at 10°C and the injection volume was 5 μL. The ionisation mode was operated in negative mode for the detection using the Dual AJS Jet stream ESI Assembly. The quadrupole time-of-flight (QTOF) acquisition settings were configured in 4 GHz high-resolution mode (resolution 17 000 full width at half maximum (FWHM) at *m/z* 1000), data storage in profile mode and the high-resolution full mass spectrometry (MS) chromatograms were acquired over the range of *m/z* 100–1700 at a rate of 3 spectra/s. The mass spectrometer was calibrated in negative mode using ESI-L solution from Agilent Technologies every 6 hours to maintain the best possible mass accuracy. Source parameters were set up as follows: drying gas flow, 8 L/min; gas temperature, 300°C; nebuliser pressure, 35 psi; capillary voltage, 3500 V; nozzle voltage, 1000 V. Data were processed afterwards using the MassHunter Quantitative software and MassHunter Qualitative software (Agilent Technologies) to control the mass accuracy for each run. In the quantitative method, 43 bile acids were quantified by calibration curves. The quantification was corrected by addition of internal standards in all samples and calibration levels. Extracted ion chromatograms were generated using a retention time window of ±1.5 min and a mass extraction window of ±60 ppm around the theoretical mass of the targeted bile acid.

For all experiments, BAs that were not detected by the respective methods were assumed to be absent, set to 0 μmol/g and only those BAs detected in at least 50% of the animals in at least one group were considered for downstream analyses. Statistics were done only on dominant BA species (the concentration thresholds are shown in the figures; all individual values for all BAs are available in online supplemental tables S2–4). Ursodeoxycholic acid (UDCA) is a primary BA in rodents, but a secondary BA in humans. Due to their similarity to humans, we classified UDCA as a secondary BA in pigs.

Lipidomic analyses

Faecal homogenates for analysis of fatty acids, sterols and stanols were prepared in isopropanol as described before.[52] Subsequently, the homogenates were used for both fatty acid and sterol/stanol analysis. Concentrations of total faecal fatty acids were determined by gas chromatography coupled to mass spectrometry (GC-MS) as described previously[53] with some modifications. Samples were derivatised to fatty acid methyl ester (FAME). The initial column temperature of 50°C was held for 0.75 min, increased with 40 °C/min to 110°C, with 6 °C/min to 210°C, with 15 °C/min to 250°C and held for 2 min. Iso-FAMEs and ante-iso-FAMEs standards were applied to identify branched chain fatty acids and to calibrate the instrument response. Samples for analysis of sterols and stanols were analysed as described previously.[54]

Generation of bacterial supernatants for organoid experiments

For the incubation of either wild-type *F. contorta* or the Ω*baiH* mutant with CA, 100 µL overnight culture was inoculated in 10 mL of trypticase soy broth supplemented with resazurin, hemin, yeast extract, salt solution, L-cysteine and 100 µM CA under anaerobic conditions. For the incubation of BACOMI with or without *C. scindens*, 100 µL overnight culture of each strain was inoculated together in 10 mL of trypticase soy broth supplemented with resazurin, hemin, yeast extract, salt solution, 1 M taurine, L-cysteine and either 50 µM DCA, or dimethyl sulfoxide (DMSO) as negative control, under anaerobic conditions. After 24 hours at 37°C, the cultures were centrifuged (16 000x g, 5 min, 4°C) and cell-free supernatants collected.

Human colonic organoid experiments

Normal colon organoids, established from healthy human intestinal biopsies, were kindly provided by Dr Franziska Baenke and Dr Daniel E Stange (Dresden, Germany). They were maintained in Matrigel (#356231, Corning) supplemented with growth medium (IntestiCult, #06010, STEMCELL Technologies, Vancouver, Canada). For growth analysis, 50 µM CA or DCA (#C1129 and #D2510, respectively; both Sigma Aldrich, Burlington, USA) or bacterial supernatants were added as indicated and the organoids were incubated for 48 hours at 37°C. Intact organoids were detached from Matrigel using Cell Recovery Solution (#CLS354253, Corning) and embedded in Epredia HistoGel (HG-4000–012, Thermo Fischer Scientific). Cells were fixed in ROTIHistofix (#P087.5, Carl Roth, Karlsruhe, Germany) for 24 hours and embedded in paraffin. Tissues were cut into 4 µm-thick sections, deparaffinised with xylol three times for 5 min, then rehydrated using a decreasing alcohol series: three times each 100%, 96% and 70% (each time for 3 min), followed by PBS three times for 5 min. Afterwards, the specimens were boiled in 10 mM citrate buffer (pH=6) for 25 min for antigen retrieval, followed by 30 min of cooling. Thereafter, the specimens were washed three times with PBS for 5 min, and then blocked with PBS containing

Gut: first published as 10.1136/gutjnl-2024-332243 on 18 December 2025. Downloaded from http://gut.bmj.com/ on November 19, 2026 by guest. Protected by copyright, including for uses related to text and data mining, AI training, and similar technologies.

1% bovine serum albumin and 0.2% Triton X-100 for 30 min at room temperature. Primary antibodies against Ki67 (Cell Signaling Technology, Danvers, USA, 12 202S, dilution 1:200) were incubated overnight at 4°C. Specimens were then washed three times in PBS (5 min each) and incubated with the secondary antibody (AlexaFluor-594, Thermo Fisher Scientific A21207, dilution 1:1000), and 4',6-diamidino-2-phenylindole (DAPI) (dilution 1:1000) for 1 hour at room temperature. All antibodies were diluted in PBS containing 1% bovine serum albumin. Finally, the specimens were washed in PBS for 5 min and covered with glass slides using mounting medium (DAKO FluorSave, Glostrup, Denmark). For imaging, a fluorescence Olympus IX81 microscope was used (Evident Scientific, Waltham, USA).

Data visualisation and statistics

Statistical analyses were done using R (V.4.2.1) in RStudio using the rstatix package or GraphPad Prism (V.10.6.1) (GraphPad Software, Boston, USA). For microbiota analyses, detailed information is provided in Rhea (https://github.com/Lagkouvardos/Rhea).[44] Comparisons between two groups were done by Wilcoxon tests and Benjamini-Hochberg adjustment. Comparisons between three groups were done by Kruskal-Wallis tests with Dunn's multiple comparisons and Benjamini-Hochberg adjustments. Adjusted p values are with stars as defined in the corresponding legends; non-adjusted p values are given as numbers directly in the graphs whenever appropriate. Graphs were created in R using tidyverse (ggplot2; RRID:SCR_014601), ggpubr, cowplot and ggbreak or GraphPad Prism. BioRender.com was used to create the visual abstract (Created in BioRender. Oßwald, A. (2026) https://BioRender.com/gj1ikmx).

Author affiliations
[1]Research Group WESTGUT, ZIEL - Institute for Food & Health, Technical University of Munich, Freising, Germany
[2]Gnotobiology Research Unit, German Institute of Human Nutrition Potsdam-Rehbruecke, Nuthetal, Germany
[3]Functional Microbiome Research Group, Institute of Medical Microbiology, RWTH University Hospital, Aachen, Germany
[4]Chair of Nutrition and Immunology, School of Life Sciences, Technical University of Munich, Freising, Germany
[5]Department of Internal Medicine A, University Medicine Greifswald, Greifswald, Germany
[6]Molecular Systems Biology Unit, European Molecular Biology Laboratory, Heidelberg, Germany
[7]Leiden University Center for Infectious Diseases (LUCID), Leiden University Medical Center, Leiden, The Netherlands
[8]Chair of Livestock Biotechnology, School of Life Sciences, Technical University of Munich, Freising, Germany
[9]Chair of Infections Pathogenesis, School of Life Sciences, Technical University of Munich, Freising, Germany
[10]Institute of Pharmacy, Department of Pharmacology and Toxicology, Freie Universität Berlin, Berlin, Germany
[11]Environmental Microbiology Laboratory, School of Architecture, Civil and Environmental Engineering, École Polytechnique Fédérale de Lausanne, Lausanne, Switzerland
[12]Institute of Clinical Chemistry and Laboratory Medicine, University Hospital of Regensburg, Regensburg, Germany
[13]Bavarian Center for Biomolecular Mass Spectrometry, School of Life Sciences, Technical University of Munich, Freising, Germany
[14]Institute of Food Technology and Food Chemistry, Technische Universität Berlin, Berlin, Germany
[15]The Jill Roberts Institute for Research in IBD, Department of Medicine, Weill Cornell Medicine, New York, New York, USA
[16]Department of Animal Sciences, University of Illinois Urbana-Champaign, Urbana, Illinois, USA
[17]Department of Visceral Surgery and Medicine, Inselspital, Bern University Hospital, University of Bern, Bern, Switzerland
[18]ZIEL – Institute for Food & Health, Technical University of Munich, Freising, Germany

Acknowledgements We are grateful to: (1) Viola and Steffen Loebnitz, Tatiana Flisikowska and Thomas Winogrodzky from the Chair of Livestock Biotechnology at the Technical University of Munich, Germany, for their support with pig experiments; (2) Ines Grüner, Anika Sander, Sabine Schmidt and Anke Gühler from the German Institute of Human Nutrition Potsdam-Rehbruecke, Nuthetal, Germany, for their help with the germ-free mouse colony and colonisation experiments, and Tobias Goris and Annett Braune for their critical review of data; (3) Franziska Baenke and Daniel Stange from the Department of Visceral, Thoracic and Vascular Surgery at the University Hospital Carl Gustav Carus of the Technical University of Dresden, Germany, for their support with organoids.

Contributors TC, SO, EW and AO conceived and designed the experimental approaches, supported by DW, JR, SZ and KF. SZ, DH, KF, TC and SO acquired funding for the study. AO, EW, DW, SK, OIC, KP, QRD, WL, NT, FS, CV, SM, KK, MG, SR, C-JG and GL performed experiments, established methods and created model systems. AO, EW, DW, SK, OIC, KP, QRD, WL, CV, SM, KK, MG, TC and SO performed data analysis and curation. ASt, TC and SO managed and coordinated research activities. SR, C-JG, BK, GL, ASc, RB-L, GZ, SZ, DH, KF, TC and SO provided study materials and essential resources. ASt, NT, AC, RB-L, GZ, SZ, DH, KF, TC and SO supervised research activities and experiments. AO, EW, TC and SO designed graphs and figures, and wrote the original draft of the manuscript. All authors have read and approved the final version of the manuscript. TC and SO are guarantors. TC and SO are joint last authors and share correspondence.

Funding TC received funding from the German Research Foundation (DFG): project no. 460129525 'NFDI4Microbiota' and 453229399. TC and DH received funding from the DFG: project no. 395357507 - SFB1371 'Microbiome Signatures'. TC, GZ, SZ, DH and KF received funding from the German Ministry for Research and Education (BMBF): consortium project Mi-EOCRC (01KD2102D). SO received funding from the DFG: project no. 338582098.

Competing interests None declared.

Patient and public involvement Patients and/or the public were not involved in the design, or conduct, or reporting, or dissemination plans of this research.

Patient consent for publication Not applicable.

Ethics approval We used already published data from human case–control metagenomic studies, as detailed in online supplemental table S8. The generation of human colon organoids from human intestinal biopsies was approved by the institutional ethics board of Dresden University of Technology (BO-EK-297062022). Participants gave informed consent to participate in the study before taking part. Ethical approvals for the animal studies are provided in the methods.

Provenance and peer review Not commissioned; externally peer reviewed.

Data availability statement All data relevant to the study are included in the article or uploaded as supplementary information. All data used to generate the figures is available in the supplementary tables (online supplemental tables S2–4). Raw data of the 16S rRNA gene amplicon sequencing was submitted to ENA and is available under project PRJEB60380.

Supplemental material This content has been supplied by the author(s). It has not been vetted by BMJ Publishing Group Limited (BMJ) and may not have been peer-reviewed. Any opinions or recommendations discussed are solely those of the author(s) and are not endorsed by BMJ. BMJ disclaims all liability and responsibility arising from any reliance placed on the content. Where the content includes any translated material, BMJ does not warrant the accuracy and reliability of the translations (including but not limited to local regulations, clinical guidelines, terminology, drug names and drug dosages), and is not responsible for any error and/or omissions arising from translation and adaptation or otherwise.

Open access This is an open access article distributed in accordance with the Creative Commons Attribution Non Commercial (CC BY-NC 4.0) license, which permits others to distribute, remix, adapt, build upon this work non-commercially, and license their derivative works on different terms, provided the original work is properly cited, appropriate credit is given, any changes made indicated, and the use is non-commercial. See: https://creativecommons.org/licenses/by-nc/4.0/.

ORCID iDs
Annika Osswald https://orcid.org/0000-0003-3734-4125
Fabian Schumacher https://orcid.org/0000-0001-8703-3275
Georg Zeller https://orcid.org/0000-0003-1429-7485
Dirk Haller https://orcid.org/0000-0002-6977-4085
Thomas Clavel https://orcid.org/0000-0002-7229-5595

REFERENCES

1 Bray F, Laversanne M, Sung H, *et al*. Global cancer statistics 2022: GLOBOCAN estimates of incidence and mortality worldwide for 36 cancers in 185 countries. *CA Cancer J Clin* 2024;74:229–63.
2 Keum NN, Giovannucci E. Global burden of colorectal cancer: emerging trends, risk factors and prevention strategies. *Nat Rev Gastroenterol Hepatol* 2019;16:713–32.

Gut: first published as 10.1136/gutjnl-2024-332243 on 18 December 2025. Downloaded from http://gut.bmj.com/ on November 19, 2026 by guest. Protected by copyright, including for uses related to text and data mining, AI training, and similar technologies.

3 Lichtenstein P, Holm NV, Verkasalo PK, *et al*. Environmental and heritable factors in the causation of cancer--analyses of cohorts of twins from Sweden, Denmark, and Finland. *N Engl J Med* 2000;343:78–85.
4 O'Keefe SJD, Li JV, Lahti L, *et al*. Fat, fibre and cancer risk in African Americans and rural Africans. *Nat Commun* 2015;6:1–29.
5 Ocvirk S, Wilson AS, Posma JM, *et al*. A prospective cohort analysis of gut microbial co-metabolism in Alaska Native and rural African people at high and low risk of colorectal cancer. *Am J Clin Nutr* 2020;111:406–19.
6 Hill MJ, Drasar BS, Williams REO, *et al*. FÆCAL BILE-ACIDS AND CLOSTRIDIA IN PATIENTS WITH CANCER OF THE LARGE BOWEL. *The Lancet* 1975;305:535–9.
7 Wirbel J, Pyl PT, Kartal E, *et al*. Meta-analysis of fecal metagenomes reveals global microbial signatures that are specific for colorectal cancer. *Nat Med* 2019;25:679–89.
8 Wang S, Dong W, Liu L, *et al*. Interplay between bile acids and the gut microbiota promotes intestinal carcinogenesis. *Mol Carcinog* 2019;58:1155–67.
9 Bernstein C, Holubec H, Bhattacharyya AK, *et al*. Carcinogenicity of deoxycholate, a secondary bile acid. *Arch Toxicol* 2011;85:863–71.
10 Flynn C, Montrose DC, Swank DL, *et al*. Deoxycholic acid promotes the growth of colonic aberrant crypt foci. *Mol Carcinog* 2007;46:60–70.
11 Cao H, Luo S, Xu M, *et al*. The secondary bile acid, deoxycholate accelerates intestinal adenoma–adenocarcinoma sequence in Apc min/+ mice through enhancing Wnt signaling. *Fam Cancer* 2014;13:563–71.
12 Cao H, Xu M, Dong W, *et al*. Secondary bile acid-induced dysbiosis promotes intestinal carcinogenesis. *Int J Cancer* 2017;140:2545–56.
13 Flisikowska T, Merkl C, Landmann M, *et al*. A porcine model of familial adenomatous polyposis. *Gastroenterology* 2012;143:1173–5.
14 Flisikowski K, Perleberg C, Niu G, *et al*. Wild-type APC Influences the Severity of Familial Adenomatous Polyposis. *Cell Mol Gastroenterol Hepatol* 2022;13:669–71.
15 Song M, Yang Q, Zhang F, *et al*. Hyodeoxycholic acid (HDCA) suppresses intestinal epithelial cell proliferation through FXR-PI3K/AKT pathway, accompanied by alteration of bile acids metabolism profiles induced by gut bacteria. *FASEB J* 2020;34:7103–17.
16 Zarras P, Vogl O. Polycationic salts as bile acid sequestering agents. *Prog Polym Sci* 1999;24:485–516.
17 Ruscheweyh H-J, Milanese A, Paoli L, *et al*. Cultivation-independent genomes greatly expand taxonomic-profiling capabilities of mOTUs across various environments. *Microbiome* 2022;10:212.
18 Streidl T, Karkossa I, Segura Muñoz RR, *et al*. The gut bacterium *Extibacter muris* produces secondary bile acids and influences liver physiology in gnotobiotic mice. *Gut Microbes* 2021;13:1–21.
19 Streidl T, Kumar N, Suarez LN, *et al*. Extibacter. In: *Bergey's manual of systematics of archaea and bacteria*. Wiley, 2019: 1–7.
20 Coleman OI, Lobner EM, Bierwirth S, *et al*. Activated ATF6 Induces Intestinal Dysbiosis and Innate Immune Response to Promote Colorectal Tumorigenesis. *Gastroenterology* 2018;155:1539–52.
21 Kövilein J, Sorbie A, Khaloian S, *et al*. Susceptibility to inflammatory bowel diseases promotes invasive carcinomas in a murine model of ATF6-driven colon cancer. *J Crohns Colitis* 2025;19:jjaf102.
22 Brugiroux S, Beutler M, Pfann C, *et al*. Genome-guided design of a defined mouse microbiota that confers colonization resistance against Salmonella enterica serovar Typhimurium. *Nat Microbiol* 2016;2:16215.
23 Jin W-B, Li T-T, Huo D, *et al*. Genetic manipulation of gut microbes enables single-gene interrogation in a complex microbiome. *Cell* 2022;185:547–62.
24 Pai R, Tarnawski AS, Tran T. Deoxycholic acid activates beta-catenin signaling pathway and increases colon cell cancer growth and invasiveness. *Mol Biol Cell* 2004;15:2156–63.
25 Fu T, Coulter S, Yoshihara E, *et al*. FXR Regulates Intestinal Cancer Stem Cell Proliferation. *Cell* 2019;176:1098–112.
26 Sorrentino G, Perino A, Yildiz E, *et al*. Bile Acids Signal via TGR5 to Activate Intestinal Stem Cells and Epithelial Regeneration. *Gastroenterology* 2020;159:956–68.
27 Xie G, Wang X, Huang F, *et al*. Dysregulated hepatic bile acids collaboratively promote liver carcinogenesis. *Int J Cancer* 2016;139:1764–75.
28 Kühn T, Stepien M, López-Nogueroles M, *et al*. Prediagnostic Plasma Bile Acid Levels and Colon Cancer Risk: A Prospective Study. *J Natl Cancer Inst* 2020;112:516–24.
29 Phelps T, Snyder E, Rodriguez E, *et al*. The influence of biological sex and sex hormones on bile acid synthesis and cholesterol homeostasis. *Biol Sex Differ* 2019;10:52.
30 Amos-Landgraf JM, Heijmans J, Wielenga MCB, *et al*. Sex disparity in colonic adenomagenesis involves promotion by male hormones, not protection by female hormones. *Proc Natl Acad Sci U S A* 2014;111:16514–9.
31 Chlebowski RT, Wactawski-Wende J, Ritenbaugh C, *et al*. Estrogen plus progestin and colorectal cancer in postmenopausal women. *N Engl J Med* 2004;350:991–1004.
32 Yang J, Wei H, Zhou Y, *et al*. High-Fat Diet Promotes Colorectal Tumorigenesis Through Modulating Gut Microbiota and Metabolites. *Gastroenterology* 2022;162:135–49.
33 Arthur JC, Perez-Chanona E, Mühlbauer M, *et al*. Intestinal inflammation targets cancer-inducing activity of the microbiota. *Science* 2012;338:120–3.
34 Dmitrieva-Posocco O, Wong AC, Lundgren P, *et al*. β-Hydroxybutyrate suppresses colorectal cancer. *Nature New Biol* 2022;605:160–5.
35 Ridlon JM, Devendran S, Alves JM, *et al*. The "*in vivo* lifestyle" of bile acid 7α-dehydroxylating bacteria: comparative genomics, metatranscriptomic, and bile acid metabolomics analysis of a defined microbial community in gnotobiotic mice. *Gut Microbes* 2020;11:381–404.
36 Afrizal A, Jennings SAV, Hitch TCA, *et al*. Enhanced cultured diversity of the mouse gut microbiota enables custom-made synthetic communities. *Cell Host Microbe* 2022;30:1630–45.
37 Lagkouvardos I, Pukall R, Abt B, *et al*. The Mouse Intestinal Bacterial Collection (miBC) provides host-specific insight into cultured diversity and functional potential of the gut microbiota. *Nat Microbiol* 2016;1:16131.
38 Burkhardt W, Rausch T, Klopfleisch R, *et al*. Impact of dietary sulfolipid-derived sulfoquinovose on gut microbiota composition and inflammatory status of colitis-prone interleukin-10-deficient mice. *Int J Med Microbiol* 2021;311:151494.
39 Just S, Mondot S, Ecker J, *et al*. The gut microbiota drives the impact of bile acids and fat source in diet on mouse metabolism. *Microbiome* 2018;6:134.
40 Klindworth A, Pruesse E, Schweer T, *et al*. Evaluation of general 16S ribosomal RNA gene PCR primers for classical and next-generation sequencing-based diversity studies. *Nucleic Acids Res* 2013;41:1–11.
41 Lagkouvardos I, Joseph D, Kapfhammer M, *et al*. IMNGS: A comprehensive open resource of processed 16S rRNA microbial profiles for ecology and diversity studies. *Sci Rep* 2016;6:33721.
42 Edgar RC. UPARSE: highly accurate OTU sequences from microbial amplicon reads. *Nat Methods* 2013;10:996–8.
43 Reitmeier S, Hitch TCA, Treichel N, *et al*. Handling of spurious sequences affects the outcome of high-throughput 16S rRNA gene amplicon profiling. *ISME Commun* 2021;1:31.
44 Lagkouvardos I, Fischer S, Kumar N, *et al*. Rhea: a transparent and modular R pipeline for microbial profiling based on 16S rRNA gene amplicons. *PeerJ* 2017;5:e2836.
45 Yoon S-H, Ha S-M, Kwon S, *et al*. Introducing EzBioCloud: a taxonomically united database of 16S rRNA gene sequences and whole-genome assemblies. *Int J Syst Evol Microbiol* 2017;67:1613–7.
46 Kim KH, Park D, Jia B, *et al*. Identification and Characterization of Major Bile Acid 7α-Dehydroxylating Bacteria in the Human Gut. *mSystems* 2022;7:e0045522.
47 Mistry J, Chuguransky S, Williams L, *et al*. Pfam: The protein families database in 2021. *Nucleic Acids Res* 2021;49:D412–9.
48 Cock PJA, Antao T, Chang JT, *et al*. Biopython: freely available Python tools for computational molecular biology and bioinformatics. *Bioinformatics* 2009;25:1422–3.
49 Reiter S, Dunkel A, Metwaly A, *et al*. Development of a Highly Sensitive Ultra-High-Performance Liquid Chromatography Coupled to Electrospray Ionization Tandem Mass Spectrometry Quantitation Method for Fecal Bile Acids and Application on Crohn's Disease Studies. *J Agric Food Chem* 2021;69:5238–51.
50 Wegner K, Just S, Gau L, *et al*. Rapid analysis of bile acids in different biological matrices using LC-ESI-MS/MS for the investigation of bile acid transformation by mammalian gut bacteria. *Anal Bioanal Chem* 2017;409:1231–45.
51 Vico-Oton E, Volet C, Jacquemin N, *et al*. Strain-dependent induction of primary bile acid 7-dehydroxylation by cholic acid. *Microbiology* [Preprint] 2022.
52 Schött H-F, Krautbauer S, Höring M, *et al*. A Validated, Fast Method for Quantification of Sterols and Gut Microbiome Derived 5α/β-Stanols in Human Feces by Isotope Dilution LC-High-Resolution MS. *Anal Chem* 2018;90:8487–94.
53 Ecker J, Scherer M, Schmitz G, *et al*. A rapid GC-MS method for quantification of positional and geometric isomers of fatty acid methyl esters. *J Chromatogr B Analyt Technol Biomed Life Sci* 2012;897:98–104.
54 Kunz S, Matysik S. A comprehensive method to determine sterol species in human faeces by GC-triple quadrupole MS. *J Steroid Biochem Mol Biol* 2019;190:99–103.

Gut: first published as 10.1136/gutjnl-2024-332243 on 18 December 2025. Downloaded from http://gut.bmj.com/ on November 19, 2026 by guest. Protected by copyright, including for uses related to text and data mining, AI training, and similar technologies.